Original Article

WIND ENGINEERING

Wind Engineering
2017, Vol. 41(3) 185–210

DOI: 10.1177/0309524X17706862
journals.sagepub.com/home/wie
SAGE

Damage mitigation techniques in wind turbine blades: A review

Md Abu S Shohag[1], Emily C Hammel[1], David O Olawale[1,2] and Okenwa I Okoli[1]

Abstract

Wind blades are major structural elements of wind turbines, but they are prone to damage like any other composite component. Blade damage can cause sudden structural failure and the associated costs to repair them are high. Therefore, it is important to identify the causation of damage to prevent defects during the manufacturing phase, transportation, and in operation. Generally, damage in wind blades can arise due to manufacturing defects, precipitation and debris, water ingress, variable loading due to wind, operational errors, lightning strikes, and fire. Early detection and mitigation techniques are required to avoid or reduce damage in costly wind turbine blades. This article provides an extensive review of viable solutions and approaches for damage mitigation in wind turbine blades.

Keywords

Wind energy, composite, wind turbine blade, damage, mitigation approaches

Introduction

The development of clean energy sources is a critical need, as serious human health and environmental health issues are on the rise. Wind energy is one of the most promising renewable energy sources that emits little to no environmental pollution. Wind turbines harness kinetic energy from the wind and convert it into electrical power. Unlike traditional power plants, wind turbines emit no greenhouse gases or air pollutants.

The US Department of Energy (DOE) reported in April 2015 that more than 4.5% of the nation's electricity is supplied by wind energy (US Department of Energy, 2015). The goal of the US DOE is to generate 20% of the nation's electricity from wind energy in 2030 (Lindenberg, 2009). Using the National Renewable Energy Laboratory's WinDS model, Short et al. (2003) demonstrated that wind energy could account for 25% of US electricity by 2050. The United States has a greater potential for wind power production, approximately 23 times larger than current electricity consumption (Lu et al., 2009). The country has over 8000 GW of available land-based wind resources that are economically viable for electricity generation (Black & Veatch, 2007). Currently, China is the world's largest wind power producing country with around 115 GW, followed by the United States as the second largest, with around 66 GW of electricity (as of 2014) (Global Wind Energy Council, 2014).

The electricity generated from wind energy can significantly contribute to the reduction of greenhouse gas (GHG) emissions, air pollution, and water consumption. The US power sector consumes more water than any other sector, including agriculture. Every year, about 22–62 trillion gallons (83–235 trillion liters (L)) of water are consumed by thermal power plants (coal, natural gas, nuclear) for cooling purposes (American Wind Energy Association, 2013). By generating 140 million megawatt-hours (MWh) of electricity, wind energy not only avoided CO_2 emissions and pollutants, but also avoided the consumption of more than 30 billion gallons of water in the United States in 2012 (American Wind Energy Association, 2013).

[1]High-Performance Materials Institute, FAMU – FSU College of Engineering, Tallahassee, FL, USA
[2]Nanotechnology Patronas Group Inc., Tallahassee, FL, USA

Corresponding author:
Okenwa I Okoli, High-Performance Materials Institute, FAMU – FSU College of Engineering, 2525 Pottsdamer Street, Tallahassee, FL 32310, USA.
Email: okoli@eng.fsu.edu

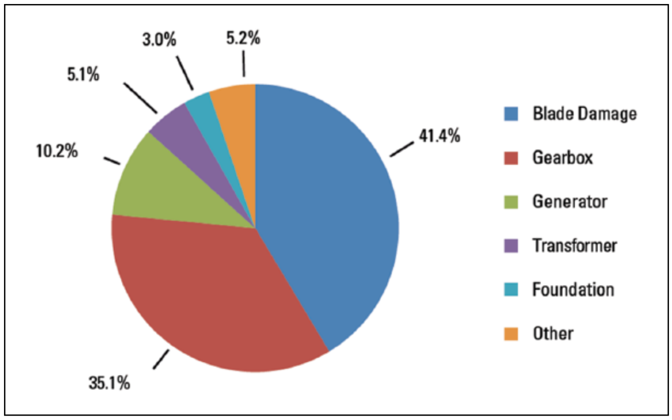

Figure 1. Most frequently reported component damage (based on number of 2012 US reported claims) (GCube Insurance Services Inc., 2012). Reprinted with permission from GCube Insurance Services Inc.

Advances in wind energy technology, yielding higher efficiency, less maintenance, and lower costs, are required for this energy source to remain competitive. Additionally, wind turbines must be able to withstand extreme environments for 20 or more years in service (Harper and Hallett, 2015; Nilsson and Bertling, 2007).

The most common type of structural damage found in wind turbines is blade damage and tower damage (Caithness Windfarm Information Forum, 2005; Ciang et al., 2008). It is reported that the wind blade had the highest number of reported damage occurrences among all other components (Figure 1) in the United States in 2012. The term "damage" can be specified as changes to the constituent material and/or geometric properties of a structure, including alterations to the boundary conditions and structural connectivity, which can negatively affect structural performance (Dongsheng et al., 2015; Farrar and Worden, 2007). Unlike aircraft or ships, wind turbines can be removed from service relatively rapidly. As a result, wind turbines are considered less safety-critical than aircraft or ships, and losses due to blade failures are primarily economic ones. Due to the number of manufacturers and processes involved in producing wind blades, there are many production-related defect types. In addition, continuous in-service inspection is quite difficult or limited because the wind blade is mostly inaccessible after installation. Thus, the safe-life design approach is recommended where the worst combination of production defects and the worst in-service damage will be considered (Hayman, 2007). Here, the safe-life design approach is used to design a structure that is able to withstand the repeated loads expected in service with consideration for turbine performance and manufacturing cost.

The cost of three blades can account for 15%–20% of the total turbine cost. As such, special attention should be given to the structural health of blades (Ciang et al., 2008; Larsen and Sorensen, 2003). The most expensive type of damage in wind turbines in terms of repair cost is the blade damage. Also the longest time is required to repair the blade damage (Larsen and Sorensen, 2003). The rotor is the highest contributor to turbine unavailability as shown in Figure 2 (Ireland, 2011). As such, appropriate damage mitigation systems are required to prevent damages in every phase of the life cycle of turbine blades starting from manufacturing steps to the operation phase. A thorough review work on damage detection methods and structural health monitoring (SHM) systems may be found in Ciang et al. (2008) and Dongsheng et al. (2015).

The major components of a wind turbine blade are illustrated in Figures 3 and 4. The constituent materials for wind turbine blades are resins, fibers, adhesives and balsa wood or rigid foam (isocyanate mixed with polyol) for the shear web. The most commonly used matrix material for the composite wind blades is epoxy resin while other resin systems such as unsaturated polyester, polyurethane, vinyl ester are also used as matrix materials. E-glass is the widely used reinforcement fiber for the current largest-sized wind blade production due to its lower cost with good mechanical performance. On the other hand, carbon fiber is a promising candidate with a stiffness five times greater than glass fiber, which reduces the tip deflection of the wind blade. The use of carbon fiber allows for the manufacture of longer blades while maintaining a comparable weight to glass fiber blades. Finally, the two shells are glued together with an adhesive which is usually epoxy.

Over the years of operation, wind turbine blades undergo severe fatigue-induced deterioration due to tremendous cyclic loads. Thus, cracks may initiate in the blades and propagate to the failure point upon certain unusual environmental factors. Among seven types of wind blade damage, delamination and adhesive joint failure are most frequent. Delaminations are the most critical and commonly studied failure mode in laminated composite materials (Abdussalam, 2000; Bolotin, 1996; Davidson et al., 2000; Elisa, 2011; Pagano and Schoeppner, 2000; Tay, 2003).

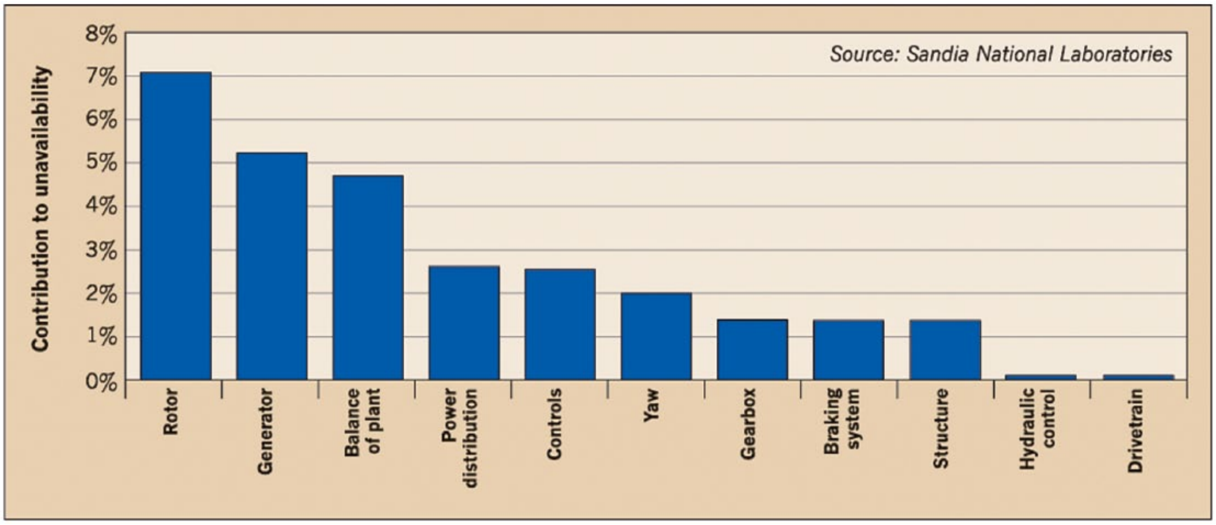

Figure 2. Wind turbine component unavailability from failure (Ireland, 2011). Reprinted with permission from EC&M.

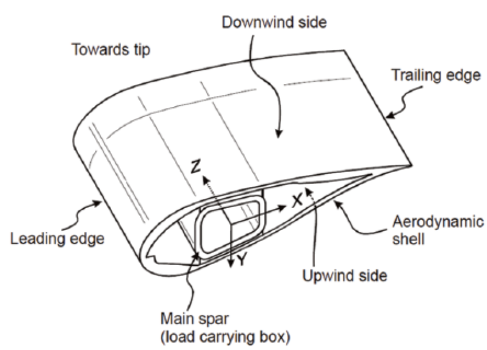

Figure 3. The main elements of a wind turbine blade (Sørensen et al., 2004).

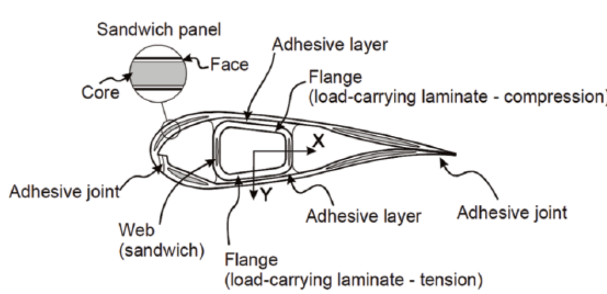

Figure 4. Nomenclature of the different blade construction elements (Sørensen et al., 2004).

There are many reasons for blade damage starting from the manufacturing floor to field operation. Usually, manufacturing-induced defects, precipitation and debris, water ingress, variable loading due to wind, operational errors, lightning strikes, and fire or even collisions with birds are accountable for the cracking and damage of wind turbine blades. Wind is the driving force of the turbine blade but wind gusts or heavy storms may damage or completely destroy the wind turbine. Wind blade failures and wind turbine accidents are compiled in Portal Energia (2014).

This review article attempts to compile the major causes of wind blade damage and their available mitigation techniques to date. Typical damage types in composite blades with their occurring locations are discussed.

Damage types in composite wind blade

Types of damage

Damage to a wind turbine blade can occur in several ways. Sørensen et al. (2004) classified seven different types of damages in their full-scale tests and post analysis of a 25-m wind turbine blade. Typical damage in turbine blades is listed in Table 1 and described pictorially in Figure 5.

Table 1. Typical damage of wind turbine blades (Ciang et al., 2008; Sørensen et al., 2004; Sundaresan et al., 2002).

Type 1	Damage formation and growth in the adhesive layer joining skin and main spar flanges (skin/adhesive debonding and/or main spar/adhesive layer debonding)
Type 2	Damage formation and growth in the adhesive layer joining the up and downwind skins along leading and/or trailing edges (adhesive joint failure between skins)
Type 3	Damage formation and growth at the interface between face and core in sandwich panels in skins and main spar web (sandwich panel face/core debonding)
Type 4	Internal damage formation and growth in laminates in skin and/or main spar flanges, under a tensile or compression load (delamination driven by a tensional or a buckling load)
Type 5	Splitting and fracture of separate fibers in laminates of the skin and main spar (fiber failure in tension; laminate failure in compression)
Type 6	Buckling of the skin due to damage formation and growth in the bond between skin and main spar under compressive load (skin/adhesive debonding induced by buckling, a specific type 1 case)
Type 7	Formation and growth of cracks in the gelcoat; debonding of the gelcoat from the skin (gelcoat cracking and gelcoat/skin debonding)

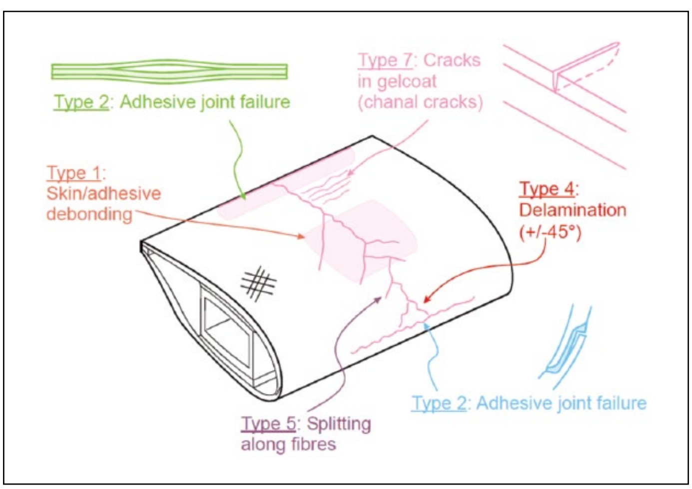

Figure 5. Different types of wind blade damages (Sørensen et al., 2004).

The post failure damage caused to the leading edge of the wind blade in laboratory experiments by Sørensen et al. (2004) is shown in Figure 6(a). Type 2 damage occurs at the leading edge. On the other hand, Figure 6(b) shows compressive load damage caused to the downwind skin at the leading edge resulting in Type 5 damage and Type 7 damage.

Damage prone regions

Ciang et al. (2008) compiled typical damage prone areas of blades: (1) 30%–35% and 70% in chord length from the blade root, (2) root section of the blade, (3) maximum chord, and (4) upper spar cap/flange of the spar. Both simulation and experimental research indicate (Ciang et al., 2008; Shokrieh and Rafiee, 2006; Sundaresan et al., 2002) that the regions along the axial locations of 30%–35% and 70% of blade length from the root section are prone to more damage. A schematic diagram showing the damage prone regions can be found in Ciang et al. (2008).

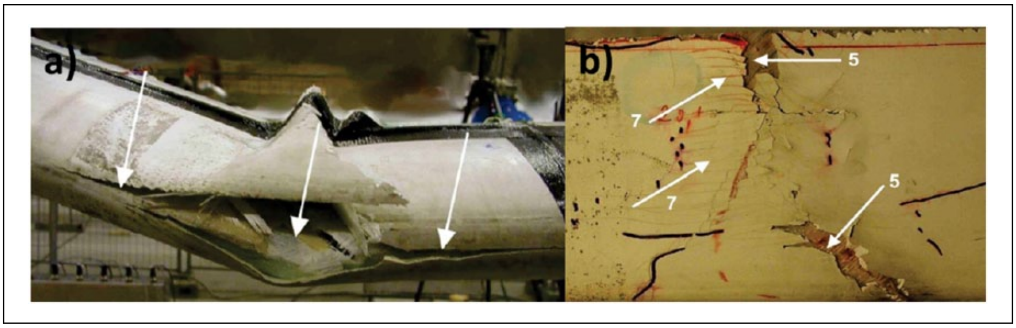

Figure 6. (a) Type 2 damage (adhesive joint failure between skins) at the leading edge (Sørensen et al., 2004) and (b) Type 5 damage (laminate failure in compression) and Type 7 damage (gelcoat cracking) at the bottom of the leading edge (Sørensen et al., 2004).

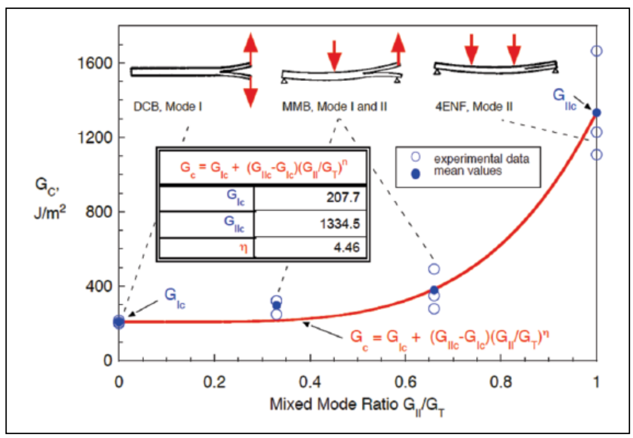

Figure 7. Mixed-mode fracture criterion for a toughened carbon/epoxy (Krueger, 2006).

Damage initiation and propagation mechanism

Over the past two decades, fracture mechanics has been widely used by researchers to characterize the onset and growth of these delaminations (O'Brien, 1982, 1998; Martin, 1998). Delamination may be attributed to incomplete curing and to interlaminar stresses created by impact (Johannesson and Blikstad, 1984). Garg (1988) showed that delamination causes localized buckling and high interlaminar shear stresses at the edges of the buckled region under compressive loading designated as instability-related delamination growth.

The growth of delamination depends upon the strain energy release rates G_I, G_{II}, and G_{III} at the crack tip. The delamination growth will occur if the total strain energy release rate, G_T, exceeds the critical value (Abdussalam, 2000), that is

$$G_T = G_I + G_{II} + G_{III} = G_C \tag{1}$$

Figure 7 shows a graph of the interlaminar fracture toughness, G_C, versus the mixed-mode ratio, G_{II}/G_T, plotted to obtain the mixed-mode fracture criterion. The fracture toughness data are generated experimentally using pure mode I ($G_{II}/G_T = 0$) Double cantilever beam (DCB), pure mode II ($G_{II}/G_T = 1$) four-point bend end-notched flexure (4ENF), and mixed-mode bending (MMB) tests for a carbon/epoxy material (Hansen and Martin, 1999). A simple mathematical relationship between G_C and G_{II}/G_T was suggested by Benzeggah and Kenane (1996) as follows

$$G_C = G_{IC} + \left(G_{IIC} - G_{IC}\right)\cdot\left(\frac{G_{II}}{G_T}\right)^{\eta} \tag{2}$$

In equation (2), G_{IC} and G_{IIC} are the experimentally determined fracture toughness data for mode I and II as shown in Figure 7. The factor η was determined by a curve fit using the Levenberg–Marquardt algorithm.

The entire failure surface $G_C = G_C (G_I, G_{II}, G_{III})$ is required in order to predict delamination initiation or growth for three-dimensional composite structures (Krueger, 2006). The failure criterion for delamination in laminated composites is greatly dependent on the mixed-mode ratio and the propagation occurs in the laminate plane (Krueger, 2004; Rybicki and Kanninen, 1977). The most commonly used method for computing the delamination growth in composite materials and structures is called the virtual crack closure technique (VCCT) (Krueger, 2004; Rybicki and Kanninen, 1977) because fracture mode separation is determined explicitly. The VCCT calculates the fracture energy at the crack tip by calculating the energy required to virtually close the crack. The work required to close all cracks are used to calculate strain energy release rates (Nelson et al., 2012). Interface elements are used to simulate crack growth (Camanho et al., 2003; Jiang et al., 2007). The growth of cracks along the interfaces between plies is found at ply drops under both static and fatigue loads (Harper and Hallett, 2015). Ply drops are common in modern large wind blades as the thickness is tapered from root to tip (Harper and Hallett, 2015).

Causes of wind blade damage

Manufacturing-induced defects

Early blade failures may occur due to manufacturing defects. The manufacturing defects may occur at random with respect to type, size, and location, and several of them are listed in the following (Cairns et al., 2011):

- Ply waviness;
- Porosity;
- Fiber misalignment;
- Delaminations;
- Debonding;
- Improper fiber/matrix distribution;
- Bonding defects;
- Foreign inclusions;
- Incompletely cured matrix;
- Matrix cracking;
- Improper fiber/resin ratio;
- Wrinkle.

These manufacturing defects contribute significantly to the reduction of the mechanical properties. Three composite material flaw types considered critical to blade function are in-plane (IP) and out-of-plane (OP) waviness, and porosity/voids (Nelson et al., 2011). Schematic diagrams of these flaw types can be found in Nelson et al. (2011). A survey conducted by Riddle et al. (2011) among wind turbine blade manufacturers, repair companies, wind farm operators, and third-party investigators shows that these are the most commonly found flaws in wind turbine blades. The static compressive strength and stiffness of laminates decrease due to the OP fiber waviness (Bogetti et al., 1994). Adams and Bell (1995) found that the compressive strength had decreased approximately 35% when investigating OP waves in a thermoplastic laminate. The static tensile strength decreases due to the presence of in-plane waves in composites, decreasing further as wave severity increases (Nelson et al., 2011). A 6%–16% strength decrease and a 2%–18% reduction in the strain at failure were found by Nelson et al. (2011) in a laminate containing 1.8% porosity. Along with above factors, others such as large resin-rich areas and resin cure variations through the thickness are more likely in larger blades (Griffin and Ashwill, 2003).

Alternatively, manufacturing defects including missing adhesive or deficient bonding may influence other parts of the wind blade such as the trailing edge. The geometrical shape of the blade and current manufacturing technique make the trailing edge of the wind turbine blade more sensitive to damage (Ataya and Ahmed, 2013). Different studies show that typical trailing edge failure is the local debonding of the adhesive joint (Eder and Bitsche, 2015; Eder et al., 2014). The main cause of trailing edge failure is missing adhesive or deficient bonding (Jüngert, 2008). The cause of this failure is complicated, with insufficient data regarding different forms of damage and failure in the trailing edge (Ataya and Ahmed, 2013; Eder and Bitsche, 2015). It is possible that other causes such as variable loading and fatigue due to operation will contribute to trailing edge failure.

Two blade lengths 9.5 m (100 kW) and 14.2 m (300 kW) were extensively analyzed to determine the type, size, and location of different forms of damage (Figures 8 and 9) (Ataya and Ahmed, 2013). Trailing edge damage is divided into following three major groups (Ataya and Ahmed, 2013):

1. Longitudinal cracks along the trailing edge through the bonding materials;
2. Transverse cracks;
3. Edge cuts or crushing.

As the inspected wind turbines are of different types (100 and 300 kW), Table 2 depicts the number of each type of damage.

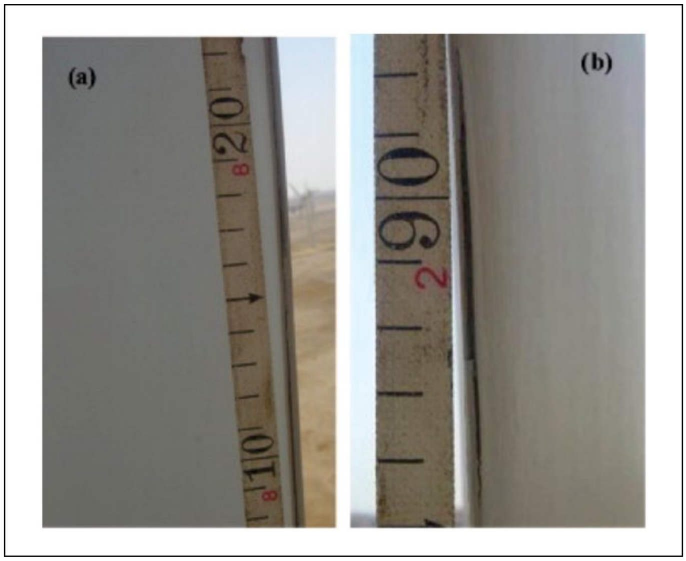

Figure 8. Examples of longitudinal cracks that found in the trailing edge of 100 kW (a) and 300 kW (b) wind turbine blades (Ataya and Ahmed, 2013). Reprinted from Ataya and Ahmed (2013). Copyright (2013), with permission from Elsevier.

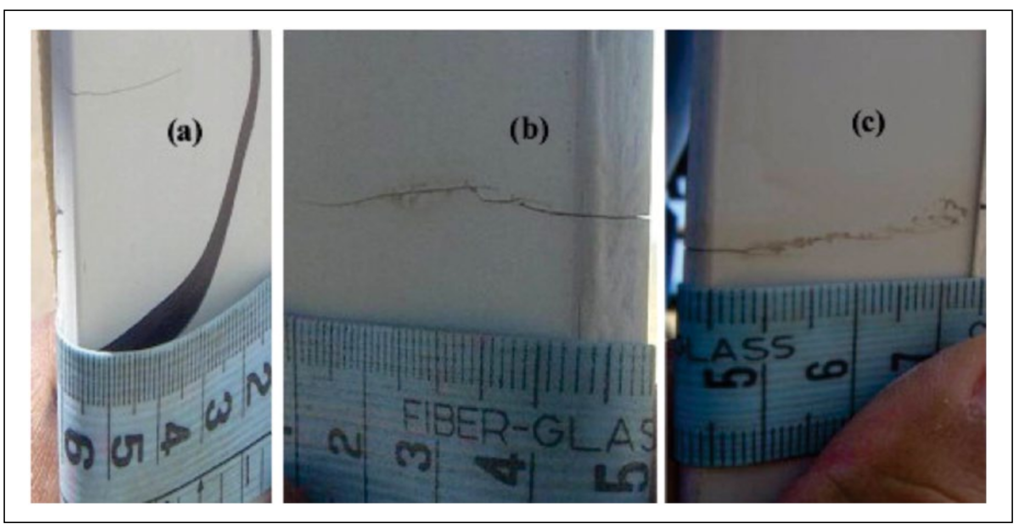

Figure 9. Examples of the simple and round transverse cracks found in the 300 and 100 kW wind turbine blades. (a) Simple TC at 0.64 of the rotor radius of a 100 kW turbine, (b) round TC at 0.82 of a 300 kW rotor radius, and (c) other side of the round TC in (b) (Ataya and Ahmed, 2013). Reprinted from Ataya and Ahmed (2013). Copyright © 2013, with permission from Elsevier.

Table 2. Number of trailing edge damage sites in the inspected wind turbine rotor blades (Ataya and Ahmed, 2013).

Discontinuities	300 kW blades	100 kW blades	Total
Longitudinal cracks	79	57	136
Transverse cracks	14	59	73
Edge cuts	43	40	83
Total	136	156	292

Precipitation and debris

Leading edge erosion. Leading edge erosion is caused by rain, hail, salt spray, and other debris (3M™, 2015). Liquid droplet impingement can cause significant blade erosion that reduces aerodynamic efficiency and hence, energy capture (Slot

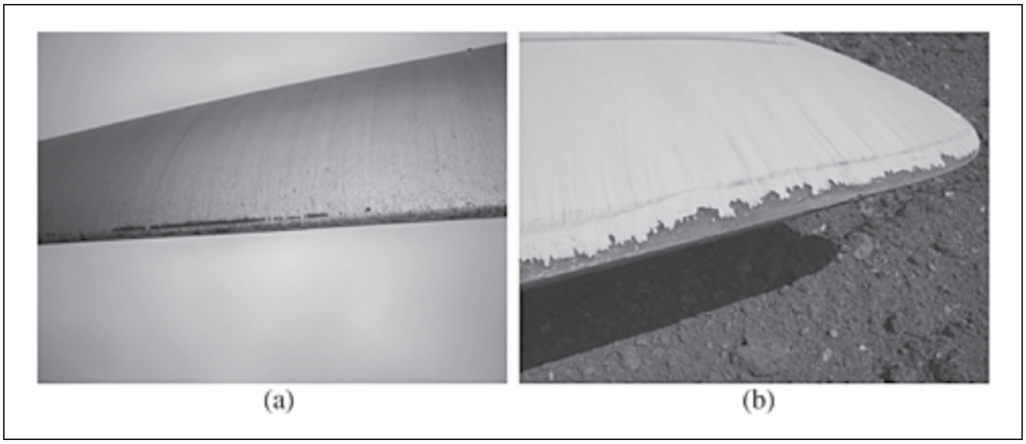

Figure 10. Photographs of wind turbine blades affected by leading edge erosion with (a) pits and gouges and (b) leading edge delamination (courtesy of 3M) (Sareen et al., 2014). From Sareen et al. (2014). Copyright © 2013, John Wiley and Sons. Reprinted by permission of John Wiley and Sons.

Figure 11. Ice accumulation and falling off on a wind turbine at Wachusett Wind Power (WindAction, 2012).

et al., 2015). Also, in the desert, wind containing sand causes leading edge erosion. This erosion can produce significant airfoil performance degradation resulting in an undesirable lift coefficient especially at the higher angles of attack (Sareen et al., 2014). Sareen et al. (2014) showed that drag could increase from 6% to 500% depending on the degree of leading edge erosion. Thus, it is predicted that annual energy production could be reduced by approximately 5% when drag increases by 80%. Figure 10(a) shows a blade with pits and gouges near the leading edge, whereas Figure 10(b) shows a much older blade with delamination over the entire leading edge (Sareen et al., 2014).

Uneven ice accretion. Ice build-up on the shell of wind blades leads to safety and operation concerns for wind farms located in cold regions. The blade exerts a heavy centrifugal force due to its high-speed rotation (tip speed could be 180 mile/h or more). The speed is quite sufficient to displace and throw accumulated ice away from the blades. Nonetheless, unequal ice accumulation on the three blades may cause unbalanced rotation that can stress the hub needlessly. In certain conditions, localization (one blade vibrates with larger amplitude than others) occurs resulting in catastrophic failure (Dongsheng et al., 2015). A 2-in-thick ice build-up on a blade surface and its consecutive projection from a blade are shown in Figure 11.

Insect contamination. Insect impact to the blade is a main source of contamination for wind turbine blades (Soltani et al., 2011). Generally, insects fly in low wind, high humidity, and temperatures above about 10°C (Corten and Veldkamp, 2001a, 2001b). At low wind speeds, the area near the stagnation line is contaminated by insects but the power is not affected because the flow near the stagnation point is very slow and also very stable and insensitive to contamination (Soltani et al., 2011). On the contrary, at higher wind speeds, the power drop is noted, although insects rarely fly in that condition. The reason behind this interesting phenomenon is the large angle of attack along the blade during high wind speeds resulting in

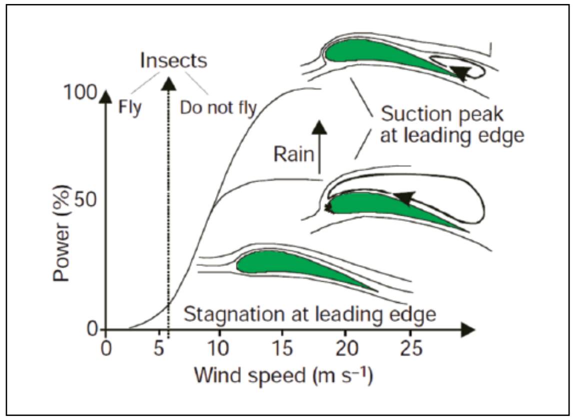

Figure 12. Illustration of the insect hypothesis proposed to explain multiple power levels (Corten and Veldkamp, 2001a). Adapted by permission from Macmillan Publishers Ltd: [NATURE] (Corten and Veldkamp, 2001a), copyright (2001).

suction peak shifts to the contaminated area (Corten and Veldkamp, 2001b; Soltani et al., 2011). Thus, the power output of turbine reduces significantly. The designed power level at higher wind speeds can be achieved after cleaning the blades or keeping the turbine operating during rains. As such, the power curve appears in different levels during operation at higher winds after operating at every low wind speeds (when insects fly) (Figure 12). This phenomenon is called multiple-power-level hypotheses (Corten and Veldkamp, 2001b).

Water ingress

Wind blades commonly experience water ingress or the permeation of moisture into the interior of the blade which can be detrimental to the performance and integrity of the wind turbine. Water enters the blades through pre-existing cracks, surface defects due to erosion, or bolted joints in the foam structure (Kithil, 2008; Nijssen and Brøndsted, 2013). Water can cause significant property degradation to the constituent components of the blade such as the resin and core materials (foam, balsa wood). The weight of the composite increases as the resin absorbs moisture. For example, composite samples from wind turbine blades were immersed into water for 90 days and a 1.66% weight increase in the composite due to the water absorption was observed (Fox, 2016). Boisseau et al. (2012) performed a study that showed a significant weight gain of glass fiber–epoxy composites when undergoing a sea water aging process at four different temperatures. The absorption of moisture affects the resin and the fiber–resin interface leading to gradual reduction of mechanical properties (Cormier and Joncas, 2010; Gurit, 2016). For a long sea water aging period, a large quasi-static strength decrease of 56% of the composite materials was observed by performing static tests (Boisseau et al., 2012). Both polyester and vinyl ester resins are more likely to degrade in water than epoxy resin due to the existence of hydrolyzable ester groups in their molecular structures (Gurit, 2016). Both weight gain and mechanical property degradation are significant at higher temperatures (>40°C) because at these temperatures, the polyester and vinyl ester based resins exhibit increasing levels of hydrolysis of the ester linkages (Hogg, 2012). Figure 13 shows the interlaminar shear strength degradation of polyester and epoxy resin thin laminates over time after immersion in water at 100°C. The results display that the polyester laminate can retain only 65% of its interlaminar shear strength, whereas an epoxy laminate immersed for the same period can retain around 90% (Gurit, 2016).

One important issue of operating wind turbines in the winter season is the durability of composite blades when used in freeze–thaw situations. The absorbed water can expand during the freeze part of the cycle and initiate microcracks in the matrix, debonding of the fiber–matrix interface, or interlaminar debonding (Hasson and Hamm, 1992). Microcracks in the matrix and fiber–matrix interface can grow and propagate under low temperature thermal cycling which eventually causes failure of the composite (Lord and Dutta, 1988; Ray, 2005). The composite can fail with multiple delaminations under the freeze–thaw conditions (Hasson and Hamm, 1992).

Variable loading due to wind

Wind turbine blades are frequently subjected to fatigue damage due to their exposure to complex systems of variable loads (Ragheb, 2009) and repetitive loads. Repetitive loads are exerted on the blades due to the continuous rotation. The weight of a blade depends on its constituent materials and length and could be 15 ton or more. With rotation, cyclical edgewise fatigue loads are exerted on the blades due to the weight of the blade itself. Wind turbine rotor blades exert varying loads

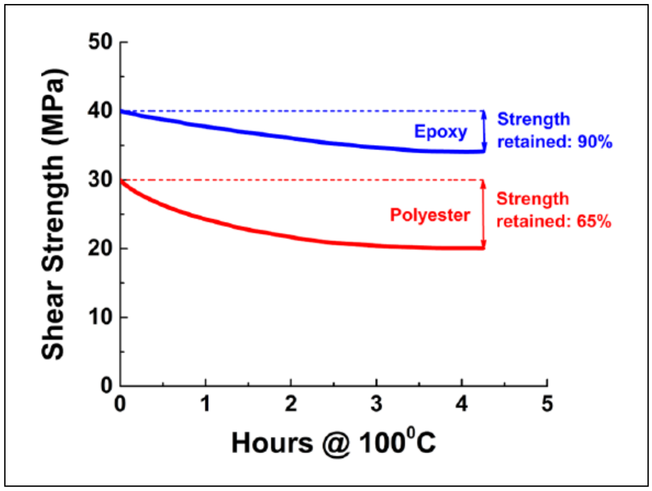

Figure 13. Effect of periods of water soak at 100°C on resin interlaminar shear strength (Gurit, 2016). Reproduced with permission from Gurit (2016).

from high wind loads (heavy storms) to lower loads especially offshore wind turbine blades. Thus, cyclic flapwise loads may induce fatigue damage evolution resulting in stable crack growth. The stable crack may become unstable crack over time potentially leading to structural failure of the rotor blade (McGugan et al., 2015). Blade failure due to fatigue loading is a very frequent problem (Mahri and Rouabah, 2002). Factors responsible for fatigue loading of wind turbine blades are (1) long and flexible structures, (2) vibrations during resonant mode, and (3) randomness in the load spectra due to the nature of wind (Spera, 1994). It has been widely reported that relatively low frequency, but high amplitude wind thrust forces, significantly contributes to fatigue damage (Ragheb, 2009). In addition, a wind gust with a sudden direction change can lead to large aerodynamic loads causing fatigue, automatic shut-downs, or even damage to some turbine components. The fatigue life of a wind blade is highly influenced by the cyclic loads that varies in the vertical direction (Manwell et al., 2010).

Operational errors

Rotor imbalances of a wind turbine can cause severe damage of the turbine components. There are two main types of rotor imbalances: mass imbalance and aerodynamic imbalances (Niebsch, 2011; Niebsch et al., 2010). The first one arises from inhomogeneous mass distributions which are caused by manufacturing errors or water inclusions in the blades' texture (Niebsch et al., 2010; Ramlau and Niebsch, 2009). The causes of manufacturing-induced errors are described in section "Manufacturing-induced defects." On the other hand, aerodynamic imbalances are mainly caused by pitch angle deviations or profile changes of the blades (Niebsch, 2011; Niebsch et al., 2010), that is, operational errors. Smaller aerodynamic imbalances due to tower shadow are not operational errors, but still contribute to noise and fatigue. The load from the aerodynamic imbalance creates vibrations and affects the drive train and might cause damage or early fatigue on other components. As a result of this imbalance, the wind attacks each blade with different force and moments. Thus, it creates vibrations and displacements on the blades primarily in axial and torsional directions with some degree of radial vibrations (Niebsch, 2011).

Lightning strike and fire

Lightning is one of the major causes of wind turbine blade damage. It can produce very short but extraordinarily high temperatures, often more than 30,000°C, by a large amount of electric current which is enough to burn the composite surface. 90% of lightning strikes to a wind turbine connect with the blade, specifically the blade tip. Repair costs could be very high, up to $30,000, and can take a couple of days to complete. The repair costs might be even larger in offshore wind blade lighting strike failure (Eritech, 2012).

Wind turbines have the following features from the viewpoint of lightning performance (Yokoyama, 2013):

1. Long turbine blades, that is, modern blades, are longer than 60 m.
2. Wind blades are made of insulated materials such as glass fiber–reinforced plastics (GFRPs) and a lightning strike can completely burn those materials.

3. Blades are rotating during power generation and this rotation may have a great impact on the number of strikes to the blades as these may be triggering their own lightning (Rachidi et al., 2008).

Lightning strikes on unprotected wind turbine blades generate a devastating internal shock wave from moisture or air expansion, or both. The high temperatures generated from lightning can force interior moisture to transit into an expansive state (steam). As a result, the excessive pressure overstresses the blade to catastrophic failure (Dongsheng et al., 2015). The lightning protection systems are discussed in section "Lightning protection methods."

Furthermore, fire is considered the second leading cause of accidents in wind turbines after blade failure (Smith, 2014). It can also completely destroy a wind turbine. The causes of fire ignition in wind turbines are mainly from lightning strikes (Andrawus et al., 2006; Starr, 2010; Uadiale et al., 2014), electrical malfunction, mechanical failure, and errors with maintenance (Smith, 2014; Starr, 2010). Braking systems in wind turbines also pose a high fire risk (Starr, 2010). Highly flammable materials (Smith, 2014; Uadiale et al., 2014) such as hydraulic oil and plastics are used in wind turbines which are normally in close vicinity to machinery and electrical wires. Overheating in these machinery or faulty electrical wires can ignite fire (Smith, 2014).

Damage mitigation techniques

Detection methods of manufacturing-induced defects

Larger structures like wind blades have a greater probability of a critical flaw than smaller structures (Cairns et al., 2011; Hertzberg, 1989). Analytical models can be used to predict the damage progression whereas different SHM techniques are used to identify the defects in service. In addition, a wide range of materials database can be used for the prediction of blade lifetime.

Progressive damage modeling. A thorough flaw characterization was performed by Riddle et al. (2011) to provide quantitative flaw data for numerical modeling programs. Elsewhere, Nelson et al. (2012) focused on the development of models that can predict the damage progression and structural implications of common defects found in composite wind turbine blades. To characterize common manufacturing defects, two distinct analytical models were investigated in Nelson et al. (2012). First, the continuum damage modeling (CDM) works under the assumption that the material is continuous and fills an entire region of space. The entire structure is broken into small elements that are called representative volume elements (RVE). The integration of the constitutive equations for RVE with respect to volume results in the total displacement, u, that reflects the equilibrium damage (equation (3)) (Nelson et al., 2012). Thus, the model indirectly displays the damage occurrence by updating the constitutive properties

$$u = \frac{1}{2}\int \varepsilon \left[C\right] \varepsilon \, dV \tag{3}$$

where $[C] = C(\varepsilon)$, C is the constitutive matrix, V is the volume, and ε is the strain. The CDM requires the homogenization of the material properties of the investigated structure. This homogenization is not always applicable when studying composites (Wang, 2001), resulting in the inability to model the exact damage. In addition, for the two different materials, damage accumulation cannot be accurately measured in some cases because it occurs independently in one of the constituents. However, to evaluate the damage accumulation in the fiber and matrix separately, simple CDMs are used in finite element analysis (Nelson et al., 2012). Progressive damage models are presented in many research publications (Chang and Chang, 1987; Chang and Lessard, 1991; Tay et al., 2005) by utilizing the material property degradation model. Second, discrete damage modeling (DDM) physically models the damage as it truly occurs in the structure. The DDM is more consistent with the physical damage characterization of thermosetting polymer-reinforced composites. Nonetheless, they are computationally more expensive and more dependent on mesh than CDM. In addition, prior knowledge of the damage location is helpful for model formulation (Nelson et al., 2012). A form of DDM is the VCCT, which is discussed in section "Damage initiation and propagation mechanism." Coupons representing progressive damage modeling of blade for IP wave have been tested and inspected by digital image correlation (DIC). The result from the DIC shows the same behavior with analytical modeling (Nelson et al., 2012).

Physical characterization approaches: SHM. Damage inspection and monitoring systems are necessary to prevent disastrous failure of wind turbine blades. SHM is used to detect damage before structural failure of wind turbine blades occurs. Some conventional SHM methods for wind turbine blades are the following: (1) visual inspection, (2) tap test, (3) X-ray radioscopy, (4) ultrasonic scanning, (5) infrared thermography, (6) acoustic emission (AE), (7) optical fiber–based approach, (8) electro-mechanical impedance–based method, and (9) piezoelectric transducers (Song et al., 2013). Niezrecki et al. (2014) performed fatigue tests on a 9-m CX-100 wind turbine blade and embedded wave defects in the spar cap laminates. Several state-of-the-art SHM approaches such as DIC, shearography, acoustic emission, fiber optic strain sensors, thermal imaging, and lead zirconate titanate (PZT) sensors were used to detect and measure the growth of flaws. Among these sensing techniques, DIC, shearography, and thermal imaging were able to clearly identify the embedded defects location and subsequent cracking (Niezrecki et al., 2014).

Composite materials fatigue database. A large Composite Materials Fatigue Database consisting over 4500 coupons for over 130 material systems was developed by the Montana State University Composites Group (MSUCG) that can be useful because most of the material systems and defect types tested are generally found in composite blades. The database contains a detailed analysis of the static and fatigue properties of a wide range of materials that was tested under a variety of loading conditions (Mandell et al., 2002; Mandell and Samborsky, 1997).

Trailing edge failure prevention methods

Surface treatment. The adhesive joint's behavior relies on coupled parameters such as geometry, hygrothermal behavior, mechanical properties, and type of singularity (Eder et al., 2014). The trailing edge laminates are glued with adhesives at an acute angle, which causes stress singularities. Perhaps, these stress singularities are responsible for initiating bond failure of the adhesive trailing edge joint. The effects of surface preparation, adhesive properties, joint configuration, and environmental factors on the adhesively bonded joints of FRP composite structures are described in Banea and Da Silva (2009). The surfaces play an important role in governing the quality of adhesive joints and the mechanical strength of the joint can be increased by surface treating the adherends prior to the application of adhesive. Surface treatment can increase surface tension and surface roughness, change surface chemistry, and thus increase bond strength and durability (Banea and Da Silva, 2009).

Appropriate materials selection. Careful selection of adhesive for trailing edge can reduce the failure in joints. Epoxy is generally used as an adhesive bond material by most of the commercial wind turbine blade manufacturers (Canales, 2008). Epoxy offers better mechanical properties, especially tensile and flexural strength, for longer blades. Polyurethane is also used to adhesively join wind turbine blades. Advantages over epoxy are faster curing (even at room temperature), low exothermal release, and excellent wetting bonding paste with a high flexibility in controlling reaction time.

Fracture toughness enhancement. The fracture strength of adhesive joints in a composite depends on the following factors: adhesive type, cure cycle, bondline thickness, adherend type, and so on (Banea and Da Silva, 2009). A team consisting of Bayer MaterialScience, the US DOE, and Molded Fiber Glass Companies invented a new reinforcement technology for polyurethane composites. By utilizing this innovative technology, the fracture toughness of polyurethane composites has been improved by 48%, which is two times that of epoxy (NetComposites, 2011). Delamination resistance of composite laminates depends on the fracture toughness of the resin matrix (Jacob et al., 2009). The fracture toughness of epoxy resin can be improved using toughening agents (Jacob et al., 2009) such as liquid rubbers (Sultan and McGarry, 1973), carboxyl-terminated butadiene nitrile rubbers (CTBN) (Pearson and Yee, 1986), core–shell particles (Lin and Shieh, 1998; Sue et al., 1994), and glass bead filling (Lee and Yee, 2000, 2001). Also, the fracture energy of epoxy resin increases significantly when pre-reacted urethane microspheres are incorporated (Okamatsu and Ochi, 2002).

Eder and Bitsche (2015) performed fracture analysis of adhesive joints in wind turbine blades. The adhesive used in a wind blade is brittle in nature, and the fracture process in trailing edges is extremely intricate. They performed experiments on adhesively bonded small-scale subcomponents and the results from those experiments were utilized to develop a numerical failure prediction of large-scale models. One of their findings is that buckling-driven debonding of adhesive trailing edge joints led to unstable crack propagation. They suggested to use interface layups which act as fiber bridging resulting in increased fracture toughness.

Predictive methodologies. Different predictive methodologies can be used to determine stresses and strains under a given loading, and to predict the probable points of failure, resulting in more efficient use of composites and adhesives. Three techniques, namely, the continuum mechanics approach (stress based), fracture mechanics, and damage mechanics approach, are used presently to predict strength of adhesively bonded joints. Nonetheless, a precise strength prediction method is required to reduce the number of costly tests at the design phase (Banea and Da Silva, 2009).

In addition, the state-of-art sensor technology can be used to predict the bond failure of the adhesive joint in wind blades. Shohag et al. (2016) proposed a novel sensing system called the in-situ triboluminescent optical fiber (ITOF)

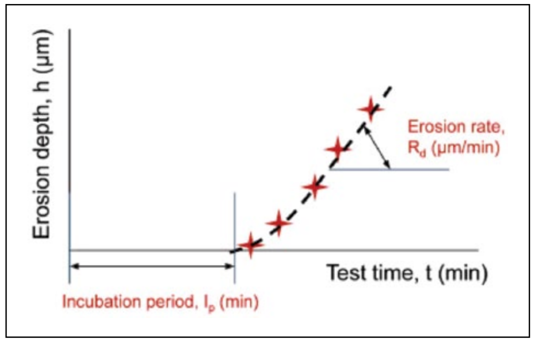

Figure 14. Schematic representation of impingement wear showing the incubation period and the stage with a constant erosion rate (Slot et al., 2015). Reprinted from Slot et al. (2015). Copyright © 2015, with permission from Elsevier.

sensor for monitoring the initiation and propagation of disbonds in composite adhesive joints. It was shown in their work that ITOF sensor can detect real-time damage in adhesive joints which might otherwise be hidden.

Protection from precipitation and debris

Leading edge erosion prevention systems. The two most common techniques to creating an effective surface coating are in-mold application and post-mold application. In the first approach, a surface coating layer of material similar to the matrix material is added to the surface of the blade as part of the molding process. On the other hand, in post-mold application, surface coatings are applied after the molding process through spraying or painting with more ductile/elastic material components such as polyurethanes (Haag, 2013). In industry, these surface coatings are called "gelcoats" irrespective of material choice or application method (Keegan et al., 2013). In addition to the gelcoat, manufacturers may apply a commercially available elastomeric coating or leading edge tape product to improve the resistance of the surface to erosion (Dalili et al., 2009; Giguère and Selig, 1999; Keegan et al., 2013). Coating life is a function of the rain intensity, the droplet diameter, the fatigue properties of the coating, and the severity of the conditions (Slot et al., 2015). Springer (1976) constructed a relationship between surface fatigue properties of coatings and the incubation lifetime for liquid impingement erosion where three stages are illustrated. The first stage is the incubation period where the surface remains unaffected, the second stage is the steady-state erosive wear stage in which surface wears at a higher rate, and the final stage is the erosion stage with strongly reduced wear rate due to higher surface roughness. Figure 14 depicts the first two stages based on the erosion depth as a function of time.

The rain erosion incubation period is considered as an estimate for the coating life that can be calculated from the following equation (Slot et al., 2015)

$$I_p = \frac{(m-1)\left(h_{tot} S_f\right)^m}{C_1 (A)^2} \frac{1}{\left[S_{\max(r_0)}^{(m-1)} - h_{tot} S_D^{(m-1)}\right]} \tag{4}$$

where $A = f(\upsilon_d, d_d, (\rho \cdot c)_{coating}), C_1 = 12(I_r / d_d)$, I_r is the rain intensity, d_d is the water drop diameter, m is the material parameter, h is the erosion depth, S_{max} is the local maximum stress level, υ_d is the water drop impact velocity, and $(\rho \cdot c)_{coating}$ is the material acoustic properties of the coating.

The polyurethane and fluorocarbon coatings were extensively studied in Schmitt (1968, 1973) for protection of aircraft radomes and composite surfaces. Some other brittle polymeric coatings such as epoxies, polyesters, silicones, and acrylics fail by brittle rupture of the coating very rapidly upon impact (Schmitt, 1973). Jilbert and Field (2000) showed that the combined effect of sand and rain erosion severely affect coating life. Further study on this combined effect for the zinc sulfide window material was conducted by Kelly et al. (1997).

3M commercialized two-component polyurethane coating (Powell, 2011) for wind blade protection from leading edge erosion. It provides excellent erosion protection.

Ice accretion prevention. Ice accumulation on wind turbine blades is detrimental to turbine performance, safety, and durability (Dalili et al., 2009). Predictive models can provide sufficient data on the ice growth rate and then suitable icing mitigation systems will be applied to remove the ice.

Ice accumulation prediction models. Physical mesoscale models such as Mesoscale Model 5 (MM5), Mesoscale Compressible Community (MC2), and others can be used to forecast icing events, although generally they are used in regional weather prediction. Empirical or statistical models which consider additional parameters such as temperature, wind direction, wind speed, cloud height are able to provide information about the amount and rate of icing (Laakso et al., 2003). The most widely used model for ice accumulation is Makkonen's (2000) algorithm

$$\frac{dM}{dt} = \alpha_1 \alpha_2 \alpha_3 w \upsilon A \tag{5}$$

where dM/dt is the maximum growth rate of icing per unit projection area of the object, α_1 is the collision efficiency, α_2 is the sticking efficiency, α_3 is the accretion efficiency, w is the mass concentration, υ is the particle velocity relative to the object, and A is the cross-sectional area relative to the particle velocity. The limitation of the model is that it is based on a cylinder. To convert the ice load to a geometrically complex structure such as a wind blade from an ideal cylinder is computationally expensive. Pallarol et al. (2014) suggested that one needs to break down the structure into small elements to model ice accretion on wind blades and should consider shadowing effects from other elements and ice growing elements together to form a single element. Again, the model requires the values of the liquid water content (LWC) of the air, the cloud droplet density, and the median volume droplet size (MVD) in the air but the problem is that there is no satisfactory method to measure these parameters nor are they routinely measured (Pallarol et al., 2014).

Icing mitigation systems. Icing mitigation systems are divided into two main categories: anti-icing and de-icing systems (ADIS). Anti-icing prevents ice from accumulating on the blade surface while de-icing removes the ice layer from the blade surface (Parent and Ilinca, 2011). Both mitigation approaches are divided into two methods: passive and active. Active methods require an energy supply and use external systems such as thermal, chemical or pneumatic, while passive methods have the advantage of utilizing the physical properties of the blade surface to eliminate or prevent ice (Dalili et al., 2009). The various icing mitigation systems with their advantages and disadvantages are listed in Tables 3 and 4.

Kimura et al. (2003) suggested a combination of coatings and active ADIS for preventing ice accretion. Currently, the available method is the passive method of special coating with active heating elements that have been tested for more than 20 years. It is simple and shows higher efficiency around 100% because it involves direct warming of the blades (Parent and Ilinca, 2011).

Insect contamination removal

Multiple-power-level hypotheses. Insect contamination in leading edge of wind blade can cause a significant power loss (Wilcox and White, 2015). To experimentally validate the multiple-power-level hypotheses, two types of blades were considered: (1) leading edge cleaned and (2) leading edge artificial roughened by a zigzag tape of maximum thickness of 1.15 mm (Corten, 2001; Corten and Veldkamp, 2001b). At low wind speeds, power output was equal in both rough and clean turbines, but at higher winds power output was higher from the clean blades. In Corten (2001), stall flagging was used to compare airflow over clean blades with blades having artificial roughness on their leading edges. The stall-flag signals were recorded by a 25 Hz digital video camera. The images from the camera indicate that flow separation on the roughened blades was significantly increased at higher wind speeds (Corten, 2001; Corten and Veldkamp, 2001a). In addition, a time series study shows that the power at high wind speeds decreased significantly after every period of low wind speed while higher power was obtained again after the blades were cleaned either manually or by rain, as expected (Corten and Veldkamp, 2001a).

Insect removal techniques. The most common and easy solution for removing insect contamination is to wait for rainfall to wash the blades (Dalili et al., 2009). There are some cleaning machines that can be used for cleaning and polishing the blades like a car wash tunnel. The demerit of using this system is that it requires the complete stoppage of the wind turbine operation resulting in power loss (Dalili et al., 2009). Another solution for removing insect contamination is to wash blades by pumping water up through the tower and spraying it into the wind and through the blade tip. The advantage of this technique is that it can be used while the turbine is in operation. It was however suggested that applying non-stick coatings on the blade surface may be the most appropriate means of insect adhesion prevention (Dalili et al., 2009). The recent study in Wilcox and White (2015) presents a computer simulation for predicting the impingement pattern for a variety of turbine operating conditions.

Water ingress prevention

In order to prevent water ingress inside the composite blades, a protective surface coating is usually used on the outer surface of the blades. The protective surface coating is referred to as a "gelcoat" and consists of a layer of material such as polyester

Table 3. Icing mitigation systems: passive anti-icing and de-icing systems (ADIS).

ADIS	Methods	Description	Advantages	Disadvantages
Passive anti-icing system	Special coating	Ice-phobic coatings prevent ice from sticking to the surface because of their anti-adherent property (Seifert, 2003) Super-hydrophobic coatings disallow water to remain on the surface because of repulsive features (Seifert, 2003) Nanocomposite coating creates high contact angles with water (Dalili et al., 2009)	Low cost, easy blade maintenance, and a protection of the whole surface (Seifert, 2003)	Coating becomes porous after a short time and loses its ability to repel ice (Tammelin et al., 2000) Found no coating to be truly ice-phobic (Anderson and Reich, 1997)
	Black paint	Allows blade heating during daylight and is used with an ice-phobic coating (Parent and Ilinca, 2011)	Quick and significant improvement in performance (Maissan, 2002) Works well in areas with high winter solar intensity (Laakso et al., 2003) Does not overheat in the summer (Weis and Maissan, 2003)	
	Chemicals	Lower the water's freezing temperature (Patreau et al., 1998)	Mainly used during aircraft take-off (Parent and Ilinca, 2011)	Pollutant; requires special application and higher maintenance (Patreau et al., 1998) Incapable of remaining on the blade surface for a long period (Tammelin et al., 2000)
Passive de-icing system	Flexible blades	Blade flexing helps to shed the ice (Dalili et al., 2009)		Little published information (Dalili et al., 2009)
	Active pitching	Orient iced blades into the sun	Work in light icing environments (Dalili et al., 2009)	Not scientifically verified and may damage wind turbines (Parent and Ilinca, 2011)

and polyurethane. Some manufacturers use leading edge tapes for additional protection as discussed in section "Leading edge erosion prevention systems." In addition, research is ongoing to develop a superhydrophobic coating made of nanoparticles embedded in resin. Karmouch and Ross (2010) developed a process of embedding silica nanoparticles in a commercial epoxy paint to act as a water-repellant surface on wind turbine blades, forcing water to run off. Peng et al. (2012) proposed a superhydrophobic polyvinylidene fluoride (PVDF) coating on a wind turbine blade that showed excellent anti-icing capability.

Alternatively, a new blade manufacturing technology could prevent the possibility of water ingress into the blades. For instance, Siemens AG's IntegralBlade has no adhesive bonded joints and is fabricated as a seamless single-piece, thus preventing critical damage modes and water ingress (Grande, 2008). Bonded joints are typically weak points in a regular composite blade because they expose the structure to cracking, water ingress, and lightning (Grande, 2008).

Fatigue loading damage avoidance

Blade damage due to the fatigue loading is a very frequent problem. If the fatigue life of a rotating turbine blade is known, then this damage can be avoided by taking necessary action before the end of its life cycle. The fatigue estimation requires the calculation of mode shapes and frequencies and the computation of displacements and stresses acting on the blades (Mahri and Rouabah, 2002). The mode shape and frequency calculation methods are described in Mahri and Rouabah (2002), while the displacements and stresses can be calculated by solving the coupled equation (bending–torsion). Once the stresses are determined, the fatigue is estimated using Miner's (1945) rule. The Palmgren–Miner linear damage rule, that is, Miner's rule, is the accepted standard (International Electrotechnical Commission (IEC), 2004) for the fatigue analysis of wind turbines as follows

$$D = \frac{n_1}{N_1} + \frac{n_2}{N_2} + \frac{n_3}{N_3} + \cdots + \frac{n_k}{N_k} = \sum_{i}^{k} \frac{n_i}{N_i} \tag{6}$$

Table 4. Icing mitigation systems: active anti-icing and de-icing systems (ADIS).

ADIS	Methods	Description	Advantages	Disadvantages
Active anti-icing system (prevent icing)	Thermal	Resistance heating and warm air used to prevent icing	No ice accumulation Blade can be kept at −5°C and thus, save 33% of power (Mayer, 2007)	Higher energy requirement Operating temperature should be less than 50°C (Laakso and Peltola, 2005)
	Air layer	Pushed through small holes near the blades' leading and trailing edges in order to generate a layer of air around the blade surface (Dalili et al., 2009)	Deflect the majority of water droplets in the air and melt few droplets that managed to hit the surface (Dalili et al., 2009)	
	Microwave	Generates heat with microwaves to prevent ice formation on blade surface (Mayer, 2007) Cover blade surface with a material that reflects microwaves (Mayer, 2007)	Tested LM19.1 blade with a 6 kW power and an emitted power less than 0.01 W/m^2 (Mansson, 2004)	Not successfully implemented yet
Active de-icing system (remove ice)	Resistance heating	Electrical heating element creates a water film between ice and blade surface and centrifugal forces throw the ice away (Battisti et al., 2006) Finnish blade heating system uses carbon fiber elements (Jasinski et al., 1998)	Requires quite small heating energy during rime accretion (Tammelin and Säntti, 1994) Higher thermal efficiency, close to 100% because of direct heating (Battisti et al., 2005)	Technology still at the prototype level (Laakso et al., 2005) Arise major imbalance on the whole system if one heater fails (Maissan, 2002) Extreme icing cases, blade heating power found insufficient (Peltola et al., 2003) Required more energy to de-ice the tip's leading edge than the hub's (Mayer et al., 2007)
	Warm air and radiator	Blow warm air into the rotor blade with special tubes to keep the blade free of ice (Laakso and Peltola, 2005; Seifert, 2003) Blowers located in the root of each blade or inside the hub Develop a water film between the ice and the surface and then centrifugal force throws the ice away (Battisti et al., 2006)	Require lower temperatures of the warm air than anti-icing system (Battisti and Fedrizzi, 2007) No negative effect on the lightning protection system or aerodynamics (Seifert, 2003) Works well in milder climates (Laakso et al., 2005)	Low thermal efficiency approx. 30% (Battisti et al., 2005) Consumes high amount of power at high wind speed and low temperature
	Flexible pneumatic boots	Inflate with compressed air to break ice (Botura and Fisher, 2003)	Works well at −10°C (Botura and Fisher, 2003) Consumes low energy (Mayer, 2007)	Affects aerodynamics by increasing drag, and cause more noise (Seifert, 2003) Requires intensive maintenance (Seifert, 2003)
	Electro impulsive/ expulsive	Electromagnetically induced vibration pulses flex a metal abrasion shield and crack the ice (Dalili et al., 2009) Magnetic field created when current is applied to the spiral coil (Mayer, 2007)	Efficient, environmentally friendly and consumes low energy (Mayer, 2007)	Not yet been tested on wind turbines (Mayer, 2007) Ice expulsion is a potential problem (Mayer, 2007)

where the total damage D is sustained by a structure that undergoes n_1 stress cycles at stress level σ_1, n_2 stress cycles at stress level σ_2, n_3 stress cycles at stress level σ_3, and so on, for all stress levels through the final level of k. N_i, the number of cycles to failure at stress level σ_i, is a measure of the material's ability to endure stress cycles. The assumption of Miner's rule is that the structure will fail when damage $D = 1$ (Sutherland, 1999).

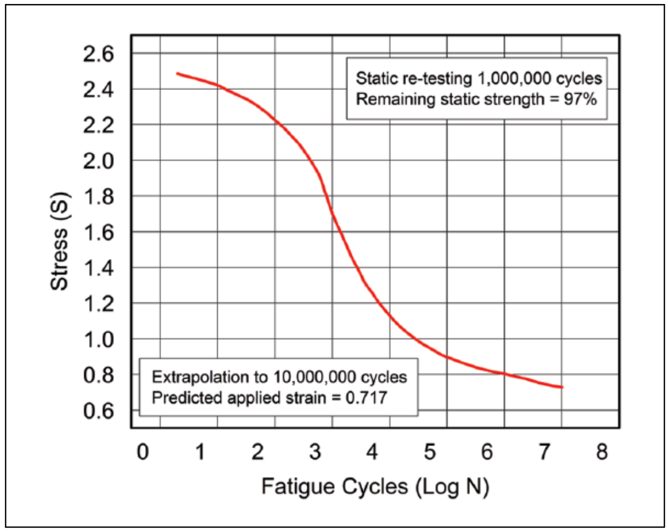

Figure 15. S-N curve for a typical wind turbine blade unidirectional material (Gurit, 2014). Reproduced with permission from Gurit (2014).

The fatigue behavior of the blade material is typically presented as a Goodman diagram in which the cycles-to-failure are plotted as a function of mean stress and range along lines of constant R-values (Sutherland, 1999). The R-value for a fatigue cycle is

$$R = \frac{\sigma_{min}}{\sigma_{max}} \tag{7}$$

where σ_{min} is the minimum stress and σ_{max} is the maximum stress in a fatigue stress cycle. A comprehensive study has been done in Sutherland and Mandell (2004) by constructing a detailed Goodman diagram for characterizing the behavior of typical fiberglass composites used in wind blades. The diagram indicates that the effect of mean stress on the prediction of damage is important and discussed in detail in Sutherland and Mandell (2004). A typical plot between the stress and the number of cycles to failure (S-N curve) is shown in Figure 15.

Freebury and Musial (2000) proposed a simplified load spectrum method using Palmgren–Miner's linear damage principles to determine equivalent-damage test loads without any specific knowledge of the test blade structure or geometry. The method does not require any conversion of load to stresses, but rather to moment, so there will be an M-N curve (applied moment vs allowable cycles to failure (Freebury and Musial, 2000)) instead of an S-N curve following the relationship below

$$M_a = M_u \times N^{\left(-\frac{1}{m}\right)} \tag{8}$$

where M_a is the amplitude moment in one load cycle, M_u is the ultimate moment of the blade, N is the allowable cycles to failure, and m is the slope of the curve.

Rotor imbalance prevention

Many defects of a turbine are related to vibrations caused by rotor imbalances. Early detection of these imbalances is required to prevent turbine damage and ensure longer life. Several algorithms and mathematical models have been developed by researchers to mitigate this problem.

Mathematical models and algorithm. Niebsch (2011) has developed a mathematical model based on blade element momentum (BEM) theory to determine imbalances from vibration measurements. In later work (Niebsch et al., 2010), Niebsch with others proposed a model that allows for a reconstruction of both mass imbalances and aerodynamic imbalance caused by deviations in pitch angles at the same time.

Furthermore, Kusnick et al. (2015) proposed an algorithm for detecting rotor imbalance and locating the problematic blades during operation. In Eric and Bayrak (2015), another algorithm was developed that can reconstruct both mass

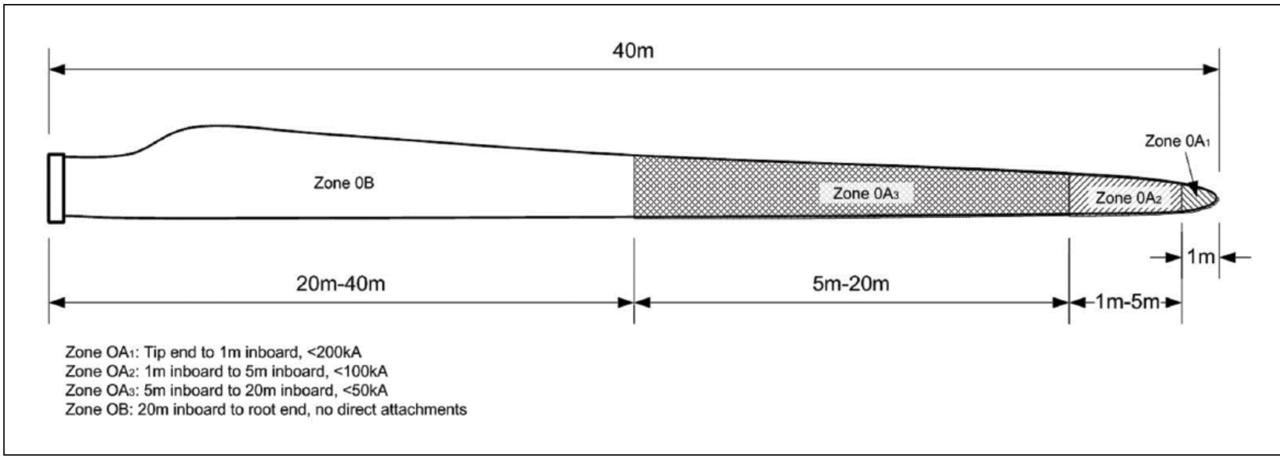

Figure 16. New zoning concept based on the expected peak current amplitudes. The distances are measured from the blade tip (Madsen et al., 2012).

imbalances and aerodynamic imbalances. The mathematical approach based on BEM method and vibration equations has been used to determine both imbalances and finally developed a reconstruction method that is implemented into a condition monitoring system.

Rotor imbalance eradication approaches. The following is the most commonly used method to detect and measure the rotor imbalances. An expert team first tries to detect aerodynamic imbalances by measuring vibrations in the radial, axial and torsional directions (Niebsch, 2011) and then uses optical methods to detect pitch angle deviation (Niebsch, 2011; Niebsch et al., 2010). After removing aerodynamic imbalances, again the remaining vibrations are measured that represent mass imbalances. The mass imbalance and its position are calculated by taking repeated measurements with placing a test mass on a distinguished blade (Niebsch, 2011). The amount of aerodynamic imbalance varies with rotor speed and wind velocity. Therefore, unlike mass imbalance, aerodynamic imbalance elimination is not possible by adding counterweights (Eric and Bayrak, 2015). Some requirements of the process are as follows: (1) expensive manpower and (2) lot of time (Niebsch, 2011; Niebsch et al., 2010).

Alternatively, to detect mass and aerodynamic imbalances, Caselitz and Giebhardt (2005) used signal processing methods as well as trend analysis to generate an alarm system. Some requirements of these methods are as follows: (1) performing learning step under faultless condition of the rotor (Ramlau and Niebsch, 2009) and (2) adaptation of the algorithms for new generations of wind energy converters (Caselitz and Giebhardt, 2005).

Lightning strike protection systems

Mathematical models. Madsen et al. (2012) observed through numerical modeling that the tip of the wind blade is more prone to lightning strikes than elsewhere on the blade. More than 90% and 99% of all lightning strikes will occur at the outermost 1 and 2 m of the blade, respectively. The following mathematical expression is described as the probability of attachment (P_{blade}) with the distance from the blade tip (d) with blades lengths of 40–80 m

$$P_{blade} = 0.4 \cdot \exp\left(-0.4 \cdot d\right) \tag{9}$$

Madsen et al. (2012) proposed a lightning protection model called new zoning concept which is designed based on the data that the blade tips experience average to high amplitude direct lightning strikes. The model divides a wind blade into four zones (Figure 16): Zone $0A_1$ (tip end to 1 m inboard, <200 kA), Zone $0A_2$ (1 m inboard to 5 m inboard, <100 kA), Zone $0A_3$ (5 m inboard to 20 m inboard, <50 kA), and Zone 0B (20 m inboard to root end, no direct attachments). The Zone $0A_1$ must be designed in such a way that it can withstand the impact from the impulse current with the highest amplitude (200 kA). It is expected that this concept will reduce the cost of the total lightning protection system by installing devices in the lightning prone regions.

Lightning protection methods. The various types of lightning protection equipped in wind turbines blades are listed as follows (IEC, 2002; Peesapati et al., 2011):

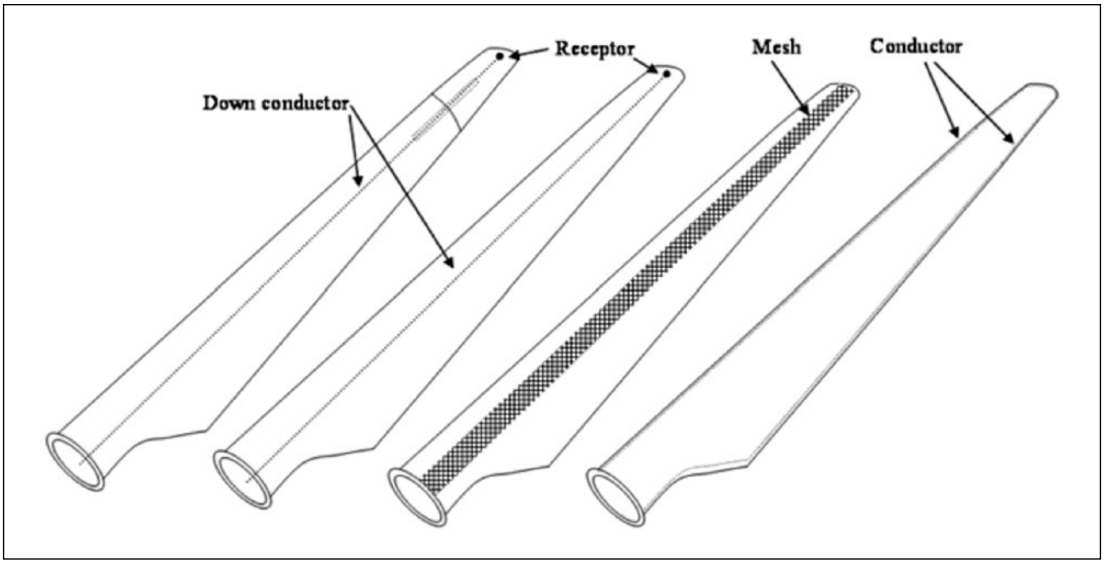

Figure 17. Lightning protection methods for rotor blades (Peesapati et al., 2011). Reprinted with permission from the Institution of Engineering and Technology.

1. Air termination systems on the blade surfaces;
2. Down conductors embedded inside the blade;
3. High resistive tapes and diverters;
4. Conducting materials incorporated into the blade surface.

The most widely used lightning protection system is the down conductor embedded along the blade length for carrying the lightning current. The receptors at the blade tip (Figure 17) act as air terminations and penetrate the blade surface (Peesapati et al., 2011). The receptors are generally made with highly conductive materials such as aluminum and copper and connected to the down conductors. As such, when lightning strikes the tip of a blade, the receptor quickly transmits the lightning current to the down conductor and then the down conductor transmits all the way to the ground. Some wind blade manufacturers have installed various types of metallic coating (aluminum or copper). But metallic coatings suffer corrosion failure because of exposure to chlorine in the marine environment. Aluminum coatings suffer pitting corrosion in chlorine-rich environment. ERICO has successfully installed a metallic lightning protection device in more than 25,000 blades globally. It developed smooth weave conductor to prevent "skin effect" (Eritech, 2012).

Radičević et al. (2012) developed a reduced-size wind turbine model where a lightning protection system in the form of receptors on the tips of the blades was experimented. They recommended that damaging effects may be reduced during bad weather accompanied by lightning and increased wind speeds by not decreasing the rotational speed of wind turbine blades (up to the critical speed). The reason behind this phenomenon is the decrease of the number of direct strikes in the zone of the air termination system on the blades with the increase of rotational speed of blades.

Sometimes, winter lightning has tremendous energy, perhaps 100 times larger than ordinary summer lightning in some cold regions. Strong winter lightning strikes are common in Japan. To protect blades from winter lightning strikes, an isolated lightning tower a little apart from the rotor hub can be used. Another suggestion is to use a long lightning rod on the nacelle to capture lightning (Naka et al., 2006).

The majority of the strikes (80%) to modern turbines are expected to be upward lightning (occurs when there is a nearby positive cloud-to-ground flash). Using carbon-reinforced plastics (CRP) for lightning strike protection in the wind blades introduces a new problem. Lightning-protection researchers and engineers should carefully consider whether CRP components are able to conduct lightning current without being damaged and the influence of the high static fields under thunderclouds on the moving carbon fiber parts. The presence of eddy currents in CRP laminates causes important energy dissipation, which might result in mechanical stresses. In order to reduce such effects, it is desirable to have two lightning down conductors (instead of one), allowing a reduction of the magnetic field inside the blade (Rachidi et al., 2008).

Further research has been done by incorporating carbon nanofibers into composite panel. By paper making process, the porous, flexible, non-woven carbon nanofiber papers (CNFP) and nickel nanostrands are prepared and then incorporated on to the surface of carbon fiber–reinforced polymer composites through resin transfer molding (RTM) process.

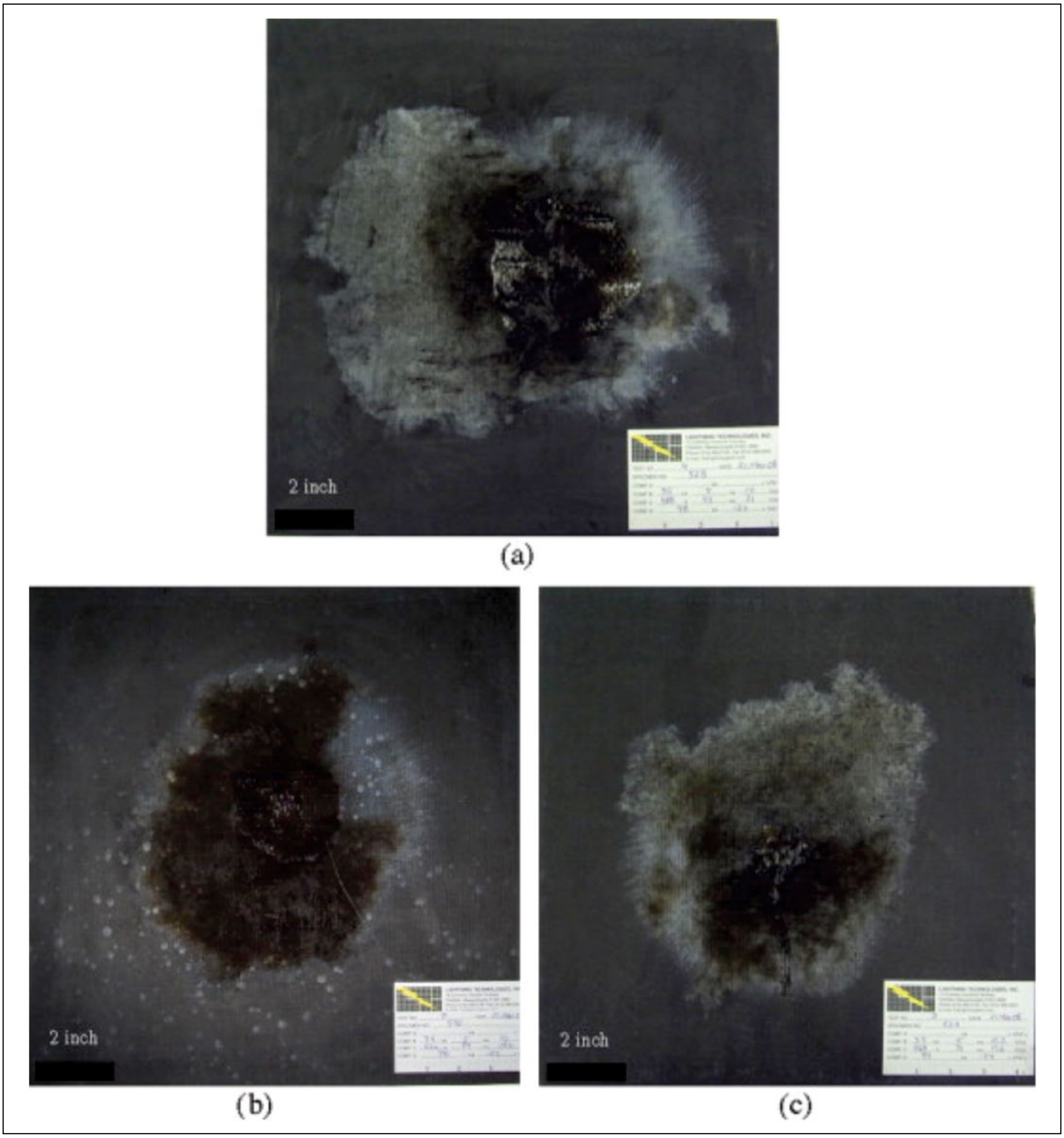

Figure 18. Surface damages of composite panels: (a) CP-CNFP-1, (b) CP-CNFP-2, and (c) CP-CNFP-3 (Gou et al., 2010). Reprinted from Gou et al. (2010). Copyright © 2010, with permission from Elsevier.

The higher the electrical conductivity of the composite panel surface, the better the lightning protection. Lightning strike tests show that CNFP-1 has maximum damaged areas while CNFP-3 has the lowest approximately 1% only (Figure 18). Nickel nanostrands are being used to increase the surface conductivity of the paper but further research is needed to put the nickel nanostrands in proper alignment (Gou et al., 2010). As the incorporation of nano-materials into composites is still in the research phase, the cost data or the cost comparison with traditional protection systems (non-nano) for an entire blade is not available. Rather roughly, the cost could be higher.

Fire prevention and control

The two methods for fire protection are passive and active. The passive methods include installing comprehensive lightning protection systems using non-combustible hydraulic and lubricant oils in wind turbine to prevent lightning strike-induced fire. It is highly recommended to use heat insulators to protect combustible materials (Smith, 2014). On the other hand, active fire protection systems include smoke alarm systems inside the turbine to alarm the fire safety authorities. Researchers also suggest suppression systems that quickly douse the flames in water or foam (Smith, 2014; Starr, 2010). Another active approach called total flooding gaseous systems can be used to protect wind turbine from fire (Starr, 2010).

Concluding remarks

Wind blades function in extreme environments and are therefore susceptible to many different damage inducing phenomena. There are seven types of wind blade damage where delamination and adhesive joint failure are most frequent. The primary causes of blade damage are manufacturing defects, precipitation and debris, water ingress, variable loading due to wind, operational errors, and lightning strike which are responsible for the mechanical properties reduction, debonding in adhesives, surface erosion and aerodynamic change, fatigue failure, or burning of the blade. Several mitigation techniques have been developed to prevent damage to wind blades. In general, mitigation techniques consist of predictive models, active and passive protection systems, and inspection methods. Accurate models can be very useful to the wind industry because damage can be predicted before failure occurs so that the costs associated with repairing the wind blades can be avoided.

Preventing wave defects during manufacturing phase is difficult because of using the large number of fiber layups for multi-megawatt turbine blades. Such kind of defects is the cause for the significant degradation of blade performance and the decrease of economic competitiveness of wind turbines. Appropriate damage modeling can predict damage progression while physical characterization techniques can quickly detect defects resulting in preventing mechanical properties reduction of the blades.

Adhesive joints in the trailing edge are prone to failure due to the stress singularities in trailing edge. Although epoxy is used by most of the blade manufacturers, polyurethane shows improved fracture toughness while incorporating a new reinforcement technology developed by a team consisting of Bayer MaterialScience, the US DOE, and Molded Fiber Glass Companies. To increase the fracture toughness of epoxy resin, liquid rubbers, CTBN, core–shell particles, glass bead filled or thermoplastic-modified epoxies can be used as toughened agents. Further research is required to invent high toughness adhesive with no compromise of mechanical and thermal properties as well as an accurate strength prediction approach of adhesively bonded joints.

Generally, gelcoats, elastomeric coating, or leading edge tape product are used to increase the resistivity of the surface to erosion. In cold regions, ice accretion on the blade surface is a big problem and detrimental to turbine performance, safety, and durability. Icing mitigation systems called ADIS can be applied to solve this problem. Advancement in coating technology is necessary to prevent blades from becoming damaged by precipitation and debris or water ingress.

Higher productivity, lower maintenance costs, and increased safety can be achieved by reducing the impact of damage inducing phenomena on the functionality of the wind blade. While several damage mitigation techniques have already been developed to address current issues, further investigation to improve damage mitigation for wind blades should be undertaken. Improvements in this area will help to ensure that wind energy will continue to be a viable source of green energy in the future.

Declaration of conflicting interests

The author(s) declared no potential conflicts of interest with respect to the research, authorship, and/or publication of this article.

Funding

The author(s) disclosed receipt of the following financial support for the research, authorship, and/or publication of this article: The authors wish to acknowledge the support of the Department of Energy under DOE Award No.: DE-NA0000728.

References

3M™ (2015) Leading edge protection. Available at: http://multimedia.3m.com/mws/media/800189O/3m-wind-erosion-solutions.pdf

Abdussalam SR (2000) *Damage and Fracture Mechanics of Composite Materials*. Winnipeg, MB, Canada: University of Manitoba.

Adams DOH and Bell SJ (1995) Compression strength reductions in composite laminates due to multiple-layer waviness. *Composites Science and Technology* 53: 207–212.

American Wind Energy Association (2013) Wind energy conserving water. Available at: http://www.awea.org/wind-and-water

Anderson DN and Reich AD (1997) *Tests of the Performance of Coatings for Low Ice Adhesion*. Washington, DC: National Aeronautics and Space Administration.

Andrawus J, Watson J, Kishk M, et al. (2006) The selection of a suitable maintenance strategy for wind turbines. *Wind Engineering* 30: 471–486.

Ataya S and Ahmed MMZ (2013) Damages of wind turbine blade trailing edge: Forms, location, and root causes. *Engineering Failure Analysis* 35: 480–488.

Banea MD and Da Silva LFM (2009) Adhesively bonded joints in composite materials: An overview. *Proceedings of the Institution of Mechanical Engineers, Part L: Journal of Materials Design and Applications 223*: 1–18.

Battisti L and Fedrizzi R (2007) 2D numerical simulation of a wind turbine de-icing system, using cycled heating. *Wind Engineering* 31: 33–42.

Battisti L, Baggio P and Fedrizzi R (2006) Warm-air intermittent de-icing system for wind turbines. *Wind Engineering* 30: 361–374.

Battisti L, Brighenti A, Dal Savio S, et al. (2005) Evaluation of anti-icing energy and power requirement for wind turbine rotors in cold climates. In: *Proceedings of the BOREAS VII conference*, Finnish Meteorological Institute (FMI), Saariselkä, 7–8 March, p. 13.

Benzeggagh M and Kenane M (1996) Measurement of mixed-mode delamination fracture toughness of unidirectional glass/epoxy composites with mixed-mode bending apparatus. *Composites Science and Technology* 56: 439–449.

Black & Veatch (2007) *Twenty Percent Wind Energy Penetration in the United States: A Technical Analysis of the Energy Resource*. Walnut Creek, CA: Black & Veatch.

Bogetti TA, Gillespie JW and Lamontia MA (1994) The influence of ply waviness with nonlinear shear on the stiffness and strength reduction of composite laminates. *Journal of Thermoplastic Composite Materials* 7: 76–90.

Boisseau A, Davies P and Thiebaud F (2012) Sea water ageing of composites for ocean energy conversion systems: Influence of glass fibre type on static behaviour. *Applied Composite Materials* 19: 459–473.

Bolotin VV (1996) Delaminations in composite structures: Its origin, buckling, growth and stability. *Composites Part B: Engineering* 27: 129–145.

Botura G and Fisher K (2003) Development of ice protection system for wind turbine applications. In: *Proceedings of the BOREAS VI conference*, Finnish Meteorological Institute (FMI), Pyhätunturi, 9–11 April, p. 16.

Cairns DS, Riddle T and Nelson J (2011) *Wind turbine composite blade manufacturing: The need for understanding defect origins, prevalence, implications and reliability*. SANDIA report SAND2011-1094, February. Albuquerque, NM: Sandia National Laboratories.

Caithness Windfarm Information Forum (2005) Wind turbine accident data to December 31st 2005. Available at: http://www.caithnesswindfarms.co.uk/

Camanho PP, Davila C and De Moura M (2003) Numerical simulation of mixed-mode progressive delamination in composite materials. *Journal of Composite Materials* 37: 1415–1438.

Canales AG (2008) *Evaluation of Bondline Thickness on Wind Turbine Blade Subcomponents*. Eindhoven: Sustainable Energy Technology Master Programme, Eindhoven University of Technology.

Caselitz P and Giebhardt J (2005) Rotor condition monitoring for improved operational safety of offshore wind energy converters. *Journal of Solar Energy Engineering: Transactions of the ASME* 127: 253–261.

Chang F-K and Chang K-Y (1987) A progressive damage model for laminated composites containing stress concentrations. *Journal of Composite Materials* 21: 834–855.

Chang F-K and Lessard LB (1991) Damage tolerance of laminated composites containing an open hole and subjected to compressive loadings: Part I—Analysis. *Journal of Composite Materials* 25: 2–43.

Ciang CC, Lee J-R and Bang H-J (2008) Structural health monitoring for a wind turbine system: A review of damage detection methods. *Measurement Science & Technology* 19: 122001.

Cormier L and Joncas S (2010) Effects of cold temperature, moisture and freeze-thaw cycles on the mechanical properties of unidirectional glass fiber-epoxy composites. In: *Proceedings of the 51st AIAA/ASME/ASCE/AHS/ASC structures, structural dynamics, and materials conference*, Orlando, FL, 12–15 April. Reston, VA: American Institute of Aeronautics and Astronautics.

Corten GP (2001) *Flow separation on wind turbines blades*. PhD dissertation, Utrecht University, Utrecht.

Corten GP and Veldkamp HF (2001a) Aerodynamics: Insects can halve wind-turbine power. *Nature* 412: 41–42.

Corten GP and Veldkamp HF (2001b) *Insects Cause Double Stall*. Petten: Netherlands Energy Research Foundation.

Dalili N, Edrisy A and Carriveau R (2009) A review of surface engineering issues critical to wind turbine performance. *Renewable & Sustainable Energy Reviews* 13: 428–438.

Davidson BD, Gharibian SJ and Yu L (2000) Evaluation of energy release rate-based approaches for predicting delamination growth in laminated composites. *International Journal of Fracture* 105: 343–365.

Dongsheng L, Siu-Chun MH, Gangbing S, et al. (2015) A review of damage detection methods for wind turbine blades. *Smart Materials and Structures* 24: 033001.

Eder MA and Bitsche RD (2015) Fracture analysis of adhesive joints in wind turbine blades. *Wind Energy* 18: 1007–1022.

Eder MA, Bitsche RD, Nielsen M, et al. (2014) A practical approach to fracture analysis at the trailing edge of wind turbine rotor blades. *Wind Energy* 17: 483–497.

Elisa P (2011) *Virtual Crack Closure Technique and Finite Element Method for Predicting the Delamination Growth Initiation in Composite Structures*. Rijeka: INTECH Open Access Publisher.

Eric N and Bayrak M (2015) Wind turbine mass and aerodynamic imbalances determination. *International Journal of Engineering Sciences & Research Technology* 4(2): 224–233.

Eritech (2012) Lightning protection for wind turbine blades. Available at: http://www.chinawind.org.cn/CWP2016/uploadpdf/1141_English.pdf

Farrar CR and Worden K (2007) An introduction to structural health monitoring. *Philosophical Transactions of the Royal Society of London Series A: Mathematical, Physical and Engineering Sciences* 365: 303–315.

Fox TR (2016) *Recycling Wind Turbine Blade Composite Material as Aggregate in Concrete*. Ames, IA: Industrial and Manufacturing Systems Engineering, Iowa State University.

Freebury G and Musial WD (2000) *Determining Equivalent Damage Loading for Full-Scale Wind Turbine Blade Fatigue Tests*. Golden, CO: National Renewable Energy Laboratory.

Garg AC (1988) Delamination—A damage mode in composite structures. *Engineering Fracture Mechanics* 29: 557–584.

GCube Insurance Services Inc. (2012) Top 5 wind energy claims. *GCube Insurance Services Inc*. Available at: http://www.gcube-insurance.com

Giguère P and Selig MS (1999) Aerodynamic effects of leading-edge tape on airfoils at low Reynolds numbers. *Wind Energy* 2: 125–136.

Global Wind Energy Council (2014) Global wind report annual market update. Available at: http://www.gwec.net/wp-content/uploads/2015/03/GWEC_Global_Wind_2014_Report_LR.pdf (accessed June 2015).

Gou J, Tang Y, Liang F, et al. (2010) Carbon nanofiber paper for lightning strike protection of composite materials. *Composites Part B: Engineering* 41: 192–198.

Grande JA (2008) Wind power blades energize composites manufacturing. *Plastics Technology*. Available at: http://www.ptonline.com/articles/wind-power-blades-energize-composites-manufacturing

Griffin DA and Ashwill TD (2003) Alternative composite materials for megawatt-scale wind turbine blades: Design considerations and recommended testing. *Journal of Solar Energy Engineering: Transactions of the ASME* 125: 515–521.

Gurit (2014) *WE Handbook-3- Structural Design*. Available at: https://www.coursehero.com/file/p35jefc/Blades-3-Gurit-2014-WE-Handbook-3-Structural-Design-Online-Available/

Gurit (2016) Guide to composites. *Support Materials*. Available at: http://www.gurit.com

Haag M (2013) Advances in leading edge protection of wind turbine blades. In: *Proceedings of the EWEA*, Vienna, 4–7 February.

Hansen P and Martin R (1999) DCB, 4ENF and MMB delamination characterisation of S2/8552 and IM7/8552. *DTIC Document*. Available at: http://oai.dtic.mil/oai/oai?verb=getRecord&metadataPrefix=html&identifier=ADA368672

Harper PW and Hallett SR (2015) Advanced numerical modelling techniques for the structural design of composite tidal turbine blades. *Ocean Engineering* 96: 272–283.

Hasson D and Hamm M (1992) *Effects of Freeze/Thaw Cycles on Hydrostatically Conditioned E-Glass/J-2 Composite*. Annapolis, MD: United States Naval Academy.

Hayman B (2007) Approaches to damage assessment and damage tolerance for FRP sandwich structures. *Journal of Sandwich Structures & Materials* 9: 571–596.

Hertzberg RW (1989) *Deformation and Fracture Mechanics of Engineering Materials*. Hoboken, NJ: John Wiley & Sons.

Hogg P (2012) Durability of wind turbine materials in offshore environments. In: *Proceedings of the SUPERGEN wind phase 2–4th training seminar, SUPERGEN Wind*, Manchester, 1 March.

International Electrotechnical Commission (IEC) (2002) *Wind turbine generator systems–Part 24: Lightning protection*. IEC TR 61400-24. Geneva: IEC. Available at: https://webstore.iec.ch/p-preview/info_iec61400-24%7Bed0.0%7Den.pdf

International Electrotechnical Commission (IEC) (2004) *Wind Turbine Generator Systems—Part 1: Safety Requirements*. Geneva: IEC.

Ireland B (2011) Preventive maintenance and troubleshooting techniques for wind turbines. Available at: http://ecmweb.com/content/wind-service

Jacob GC, Hoevel B, Pham HQ, et al. (2009) Technical advances in epoxy technology for wind turbine blade composite fabrication. In: *Proceedings of the SAMPE fall technical conference*, Wichita, KS, 19–22 October.

Jasinski WJ, Noe SC, Selig MS, et al. (1998) Wind turbine performance under icing conditions. *Journal of Solar Energy Engineering: Transactions of the ASME* 120: 60–65.

Jiang WG, Hallett SR, Green BG, et al. (2007) A concise interface constitutive law for analysis of delamination and splitting in composite materials and its application to scaled notched tensile specimens. *International Journal for Numerical Methods in Engineering* 69: 1982–1995.

Jilbert G and Field J (2000) Synergistic effects of rain and sand erosion. *Wear* 243: 6–17.

Johannesson T and Blikstad M (1984) *A fractographic study of the delamination process*. Technical report, Report from Linköping Institute of Technology. Linköping, Sweden.

Jüngert A (2008) Damage detection in wind turbine blades using two different acoustic techniques. *The NDT Database & Journal (NDT)*. Available at: http://www.ndt.net/article/v13n12/juengert.pdf

Karmouch R and Ross GG (2010) Superhydrophobic wind turbine blade surfaces obtained by a simple deposition of silica nanoparticles embedded in epoxy. *Applied Surface Science* 257: 665–669.

Keegan MH, Nash D and Stack M (2013) On erosion issues associated with the leading edge of wind turbine blades. *Journal of Physics D: Applied Physics* 46: 383001.

Kelly ES, Ondercin RJ, Detrio JA, et al. (1997) Environmental testing of long-wavelength infrared (LWIR) windows. In: *Proceedings of the SPIE 3060: Window and dome technologies and materials V*, Orlando, FL, 21 April, pp. 68–75. Bellingham, WA: SPIE.

Kimura S, Sato T and Kosugi K (2003) The effect of anti-icing paint on the adhesion force of ice accretion on a wind turbine blade. In: *Proceedings of the BOREAS VI conference*, Finnish Meteorological Institute (FMI), Pyhätunturi, 9–11 April, p. 9.

Kithil R (2008) *Case Study of Lightning Damage to Wind Turbine Blade*. Louisville, CO: National Lightning Safety Institute.

Krueger R (2004) Virtual crack closure technique: History, approach, and applications. *Applied Mechanics Reviews* 57: 109–143.
Krueger R (2006) Fracture mechanics for composites—State of the art and challenges. In: *Proceedings of the NAFEMS Nordic seminar: Prediction and modelling of failure using FEA*, Copenhagen; Roskilde, 31 May–1 June.
Kusnick J, Adams DE and Griffith DT (2015) Wind turbine rotor imbalance detection using nacelle and blade measurements. *Wind Energy* 18: 267–276.
Laakso T and Peltola E (2005) Review on blade heating technology and future prospects. In: *Proceedings of the BOREAS VII conference*, Saariselka, 7–8 March.
Laakso T, Holttinen H, Ronsten G, et al. (2003) *State-of-the-art of wind energy in cold climates*. International Energy Agency (IEA) Wind Annex XIX, p. 53.
Laasko T, Ronsten G, Tallhaug L, et al. (2005) *Wind energy projects in cold climates*. International Energy Agency (IEA) Wind Annex XIX, p. 37.
Larsen FM and Sorensen T (2003) New lightning qualification test procedure for large wind turbine blades. In: *Proceedings of the international conference on lightning and static electricity*, Blackpool, 16–19 September.
Lee J and Yee AF (2000) Role of inherent matrix toughness on fracture of glass bead filled epoxies. *Polymer* 41: 8375–8385.
Lee J and Yee AF (2001) Inorganic particle toughening I: Micro-mechanical deformations in the fracture of glass bead filled epoxies. *Polymer* 42: 577–588.
Lin K-F and Shieh Y-D (1998) Core-shell particles designed for toughening the epoxy resins. II. Core-shell-particle-toughened epoxy resins. *Journal of Applied Polymer Science* 70: 2313–2322.
Lindenberg S (2009) *20% Wind Energy by 2030: Increasing Wind Energy's Contribution to U.S. Electricity Supply*. Collingdale, PA: DIANE Publishing.
Lord HW and Dutta PK (1988) On the design of polymeric composite structures for cold regions applications. *Journal of Reinforced Plastics and Composites* 7: 435–458.
Lu X, McElroy MB and Kiviluoma J (2009) Global potential for wind-generated electricity. *Proceedings of the National Academy of Sciences 106*: 10933–10938.
McGugan M, Pereira G, Sørensen BF, et al. (2015) Damage tolerance and structural monitoring for wind turbine blades. *Philosophical Transactions of the Royal Society of London A: Mathematical, Physical and Engineering Sciences* 373: 20140077.
Madsen S, Bertelsen K, Krogh T, et al. (2012) Proposal of new zoning concept considering lightning protection of wind turbine blades. *Journal of Lightning Research* 4: 108–117.
Mahri Z and Rouabah M (2002) Fatigue estimation for a rotating blade of a wind turbine. *Revue des énergies renouvelables* 5: 39–47.
Maissan JF (2002) Wind power development in sub-arctic conditions with severe rime icing. *Northern Review* 24: 174–183.
Makkonen L (2000) Models for the growth of rime, glaze, icicles and wet snow on structures. *Philosophical Transactions of the Royal Society of London A: Mathematical, Physical and Engineering Sciences* 358: 2913–2939.
Mandell JF and Samborsky DD (1997) *DOE/MSU Composite Material Fatigue Database: Test Methods, Materials, and Analysis*. Albuquerque, NM: Sandia National Labs.
Mandell JF, Samborsky DD and Cairns DS (2002) *Fatigue of Composite Materials and Substructures for Wind Turbine Blades*. Albuquerque, NM; Livermore, CA: Sandia National Labs.
Mansson J (2004) Why de-icing of wind turbine blades. In: *Proceedings of the global windpower*, Chicago, IL, 28–31 March, p. 12. Washington, DC: American Wind Energy Association.
Manwell JF, McGowan JG and Rogers AL (2010) *Wind Energy Explained: Theory, Design and Application*. Chichester: John Wiley & Sons.
Martin R (1998) Incorporating interlaminar fracture mechanics into design. In: *Proceedings of the international conference on designing cost-effective composites, IMechE conference transactions*, London, 15–16 September, pp. 83–92.
Mayer C (2007) *Système électrothermique de dégivrage pour une pale d'éolienne*. Master's Thesis, UQAR, Rimouski, QC, Canada.
Mayer C, Ilinca A, Fortin G, et al. (2007) Wind tunnel study of electrothermal de-icing of wind turbine blades. *International Journal of Offshore and Polar Engineering* 17: 182–188.
Miner MA (1945) Cumulative damage in fatigue. *Journal of Applied Mechanics* 12: 159–164.
Naka T, Vasa NJ, Yokoyama S, et al. (2006) Experimental studies on lightning protection design for wind turbine blades. In: *Proceedings of the European Wind Energy Association (EWEC)*, Athens, 27 February–2 March.
Nelson JW, Cairns DS and Riddle TW (2011) Manufacturing defects common to composite wind turbine blades: Effects of defects. In: *Proceedings of the AIAA aerospace science meeting, wind energy symposium*, Orlando, FL, 4–7 January.
Nelson J, Cairns D, Riddle T, et al. (2012) Composite wind turbine blade effects of defects: Part B—Progressive damage modeling of fiberglass/epoxy laminates with manufacturing induced flaws. In: *Proceedings of the 53rd AIAA/ASME/ASCE/AHS/ASC structures, structural dynamics and materials conference*, Honolulu, HI, 23–26 April. Reston, VA: American Institute of Aeronautics and Astronautics.
NetComposites (2011) Polyurethane composite technology for wind turbine blades. Available at: http://netcomposites.com/news/2011/decemeber/13/polyurethane-composite-technology-for-wind-turbine-blades/
Niebsch J (2011) *Determination of Rotor Imbalances*. Rijeka: INTECH Open Access Publisher.
Niebsch J, Ramlau R and Nguyen TT (2010) Mass and aerodynamic imbalance estimates of wind turbines. *Energies* 3: 696–710.
Niezrecki C, Avitabile P, Chen J, et al. (2014) Inspection and monitoring of wind turbine blade-embedded wave defects during fatigue testing. *Structural Health Monitoring* 13: 629–643.

Nijssen RPL and Brøndsted P (2013) Chapter 6: Fatigue as a design driver for composite wind turbine blades. In: Nijssen RPL and Brøndsted P (eds) *Advances in Wind Turbine Blade Design and Materials*. Cambridge: Woodhead Publishing, pp. 175–209.

Nilsson J and Bertling L (2007) Maintenance management of wind power systems using condition monitoring systems—Life cycle cost analysis for two case studies. *IEEE Transactions on Energy Conversion* 22: 223–229.

O'Brien TK (1982) *Characterization of delamination onset and growth in a composite laminate*. *Damage in Composite Materials*, STP 775, January, pp. 140–167. West Conshohocken, PA: ASTM.

O'Brien TK (1998) Interlaminar fracture toughness: The long and winding road to standardization. *Composites Part B: Engineering* 29: 57–62.

Okamatsu T and Ochi M (2002) Effect on the toughness and adhesion properties of epoxy resin modified with silyl-crosslinked urethane microsphere. *Polymer* 43: 721–730.

Pagano N and Schoeppner G (2000) Delamination of polymer matrix composites: Problems and assessment. *Comprehensive Composite Materials* 2: 433–528.

Pallarol J, Sundén B and Wu Z (2014) On ice accretion for wind turbines and influence of some parameters. In: Amano RS and Sunden B (eds) *Aerodynamics of Wind Turbines: Emerging Topics*. Southampton: WIT Press, pp. 129–160.

Parent O and Ilinca A (2011) Anti-icing and de-icing techniques for wind turbines: Critical review. *Cold Regions Science and Technology* 65: 88–96.

Patreau V, Morency F and Paraschivoiu I (1998) Analysis of thermal de-icing system for horizontal axis wind turbine blade. In: *Proceedings of the BOREAS IV conference*, Finnish Meteorological Institute (FMI), Hetta, pp. 222–235.

Pearson RA and Yee AF (1986) Toughening mechanisms in elastomer-modified epoxies. *Journal of Materials Science* 21: 2475–2488.

Peesapati V, Cotton I, Sorensen T, et al. (2011) Lightning protection of wind turbines—A comparison of measured data with required protection levels. *IET Renewable Power Generation* 5: 48–57.

Peltola E, Laakso T, Antikainen P, et al. (2003) Prevention of icing effects. In: *Proceedings of the BOREAS VI conference*, Finnish Meteorological Institute (FMI), Pyhätunturi, p. 9.

Peng C, Xing S, Yuan Z, et al. (2012) Preparation and anti-icing of superhydrophobic PVDF coating on a wind turbine blade. *Applied Surface Science* 259: 764–768.

Portal Energia (2014) Wind turbine accident compilation. Available at: http://www.portal-energia.com/downloads/resumo-acidentes-aerogeradores-parques-eolicos.pdf

Powell S (2011) 3M™ wind blade protection coating W4600. *Industrial Marketing Presentation*.

Rachidi F, Rubinstein M, Montanya J, et al. (2008) A review of current issues in lightning protection of new-generation wind-turbine blades. *IEEE Transactions on Industrial Electronics* 55: 2489–2496.

Radičević BM, Savić MS, Madsen SF, et al. (2012) Impact of wind turbine blade rotation on the lightning strike incidence—A theoretical and experimental study using a reduced-size model. *Energy* 45: 644–654.

Ragheb M (2009) Fatigue loading wind turbines. Available at: http://mragheb.com/NPRE%20475%20Wind%20Power%20Systems/Fatigue%20Loading%20in%20Wind%20Turbines.pdf

Ramlau R and Niebsch J (2009) Imbalance estimation without test masses for wind turbines. *Journal of Solar Energy Engineering: Transactions of the ASME* 131: 011010.

Ray BC (2005) Freeze–Thaw response of glass–Polyester composites at different loading rates. *Journal of Reinforced Plastics and Composites* 24: 1771–1776.

Riddle TW, Cairns DS and Nelson JW (2011) Characterization of manufacturing defects common to composite wind turbine blades: Flaw characterization. In: *Proceedings of the 52nd AIAA/ASME/ASCE/AHS/ASC structures, structural dynamics and materials conference*, Denver, CO, 4–7 April.

Rybicki EF and Kanninen M (1977) A finite element calculation of stress intensity factors by a modified crack closure integral. *Engineering Fracture Mechanics* 9: 931–938.

Sareen A, Sapre CA and Selig MS (2014) Effects of leading edge erosion on wind turbine blade performance. *Wind Energy* 17: 1531–1542.

Schmitt GF Jr (1968) *Polyurethane Coatings for Rain Erosion Protection* (DTIC document). Fort Belvoir, VA: Defense Technical Information Center.

Schmitt GF (1973) *Advanced Rain Erosion Resistant Coating Materials*, vol. 18 (Science of Advanced Materials and Process Engineering Series). Society for the Advancement of Material and Process Engineering, pp. 57–75.

Seifert H (2003) Technical requirements for rotor blades operating in cold climate. In: *Proceedings of the BOREAS VI conference*, p. 13.

Shohag MAS, Hammel EC, Olawale DO, et al. (2016) Adhesive bond failure monitoring with triboluminescent optical fiber sensor. In: *Proceedings of the SPIE 9803: sensors and smart structures technologies for civil, mechanical, and aerospace systems*, Las Vegas, NV, 20 March, paper no. 98034Y.

Shokrieh MM and Rafiee R (2006) Simulation of fatigue failure in a full composite wind turbine blade. *Composite Structures* 74: 332–342.

Short W, Blair N, Heimiller D, et al. (2003) *Modeling the Long-Term Market Penetration of Wind in the United States*. Golden, CO: National Renewable Energy Laboratory.

Slot H, Gelinck E, Rentrop C, et al. (2015) Leading edge erosion of coated wind turbine blades: Review of coating life models. *Renewable Energy* 80: 837–848.

Smith C (2014) *Fires Are Major Cause of Wind Farm Failure, According to New Research* (21 July 2014 edition). London: Imperial College London.

Soltani MR, Birjandi AH and Seddighi Moorani M (2011) Effect of surface contamination on the performance of a section of a wind turbine blade. *Scientia Iranica* 18: 349–357.

Song G, Li H, Gajic B, et al. (2013) Wind turbine blade health monitoring with piezoceramic-based wireless sensor network. *International Journal of Smart and Nano Materials* 4: 150–166.

Sørensen BF, Jørgensen E, Debel CP, et al. (2004) *Improved design of large wind turbine blade of fiber composites based on studies of scale effects* (phase 1). Summary report, Risø-R-1390(EN), September. Roskilde: Risø National Laboratory.

Spera D (1994) *Wind Turbine Technology*. New York: ASME Press.

Springer GS (1976) *Erosion by Liquid Impact*. New York: John Wiley & Sons.

Starr S (2010) Turbine fire protection. *Wind Systems*. Available at: http://www.windsystemsmag.com/article/detail/136/turbine-fire-protection

Sue HJ, Bertram JL, Garcia-Meitin EI, et al. (1994) Fracture behavior of core-shell rubber-modified crosslinkable epoxy thermoplastics. *Colloid and Polymer Science* 272: 456–466.

Sultan JN and McGarry FJ (1973) Effect of rubber particle size on deformation mechanisms in glassy epoxy. *Polymer Engineering and Science* 13: 29–34.

Sundaresan M, Schulz M and Ghoshal A (2002) *Structural health monitoring static test of a wind turbine blade*. Subcontract report NREL/SR-500-28719, March. Golden, CO: National Renewable Energy Laboratory.

Sutherland HJ (1999) *On the Fatigue Analysis of Wind Turbines*. Livermore, CA; Albuquerque, NM: Sandia National Labs.

Sutherland HJ and Mandell JF (2004) Effect of mean stress on the damage of wind turbine blades. *Journal of Solar Energy Engineering: Transactions of the ASME* 126: 1041–1049.

Tammelin B and Säntti K (1994) Effect of rime accretion on wind energy production in the top areas of fells. In: *Proceedings of the II BOREAS conference*, Finnish Meteorological Institute (FMI), Pyhätunturi, pp. 265–275.

Tammelin B, Böhringer A, Cavaliere M, et al. (2000) Wind energy production in cold climate (WECO). Final report, Finnish Meteorological Institute, Helsinki, 1 January 1996–31 December 1998.

Tay TE (2003) Characterization and analysis of delamination fracture in composites: An overview of developments from 1990 to 2001. *Applied Mechanics Reviews* 56: 1–32.

Tay TE, Tan VBC and Tan SHN (2005) Element-failure: An alternative to material property degradation method for progressive damage in composite structures. *Journal of Composite Materials* 39: 1659–1675.

Uadiale S, Urban E, Carvel R, et al. (2014) Overview of problems and solutions in fire protection engineering of wind turbines. *Fire Safety Science* 11: 983–995 (also published in *Proceedings of the 11th symposium on International Association for Fire Safety Science*).

US Department of Energy (2015) *Wind Vision: A New Era for Wind Power in the United States*. Washington, DC: US Department of Energy.

Wang L (2001) *Effects of in-plane fiber waviness on the properties of composite materials*. MS Thesis, Department of Chemical Engineering, Montana State University, Bozeman, MT.

Weis TM and Maissan J (2003) *The Effects of Black Blades on Surface Temperatures for Wind Turbines*. Pembina Institute, Université du Québec à Rimouski.

Wilcox B and White E (2015) Computational analysis of insect impingement patterns on wind turbine blades. *Wind Energy*19: 483–495.

WindAction (2012) Industrial wind action. Available at: http://www.windaction.org/

Yokoyama S (2013) Lightning protection of wind turbine blades. *Electric Power Systems Research* 94: 3–9.